BULK ANTIBODIES for in vivo RESEARCH
α-PD-1 α-PD-L1 α-CTLA4 α-LAG3 α-4-1BB Many more!
BioCell

The Journal of Immunology

Osteopontin Promotes Protective Antigenic Tolerance against Experimental Allergic Airway Disease

This information is current as of January 17, 2018.

Themis Alissafi, Evangelia Kourepini, Davina C. M. Simoes, Nikolaos Paschalidis, Maria Aggelakopoulou, Tim Sparwasser, Louis Boon, Hamida Hammad, Bart N. Lambrecht and Vily Panoutsakopoulou

J Immunol published online 12 January 2018
http://www.jimmunol.org/content/early/2018/01/12/jimmunol.1701345

Supplementary Material http://www.jimmunol.org/content/suppl/2018/01/12/jimmunol.1701345.DCSupplemental

Why *The JI*?

- **Rapid Reviews! 30 days*** from submission to initial decision
- **No Triage!** Every submission reviewed by practicing scientists
- **Speedy Publication!** 4 weeks from acceptance to publication

**average*

Subscription Information about subscribing to *The Journal of Immunology* is online at: http://jimmunol.org/subscription

Permissions Submit copyright permission requests at: http://www.aai.org/About/Publications/JI/copyright.html

Email Alerts Receive free email-alerts when new articles cite this article. Sign up at: http://jimmunol.org/alerts

The Journal of Immunology is published twice each month by
The American Association of Immunologists, Inc.,
1451 Rockville Pike, Suite 650, Rockville, MD 20852
Copyright © 2018 by The American Association of Immunologists, Inc. All rights reserved.
Print ISSN: 0022-1767 Online ISSN: 1550-6606.

Downloaded from http://www.jimmunol.org/ by guest on January 17, 2018

Published January 12, 2018, doi:10.4049/jimmunol.1701345

Osteopontin Promotes Protective Antigenic Tolerance against Experimental Allergic Airway Disease

Themis Alissafi,*,†,1 Evangelia Kourepini,*,1 Davina C. M. Simoes,*,1 Nikolaos Paschalidis,* Maria Aggelakopoulou,* Tim Sparwasser,‡ Louis Boon,§ Hamida Hammad,† Bart N. Lambrecht,† and Vily Panoutsakopoulou*

In the context of inflammation, osteopontin (Opn) is known to promote effector responses, facilitating a proinflammatory environment; however, its role during antigenic tolerance induction is unknown. Using a mouse model of asthma, we investigated the role of Opn during antigenic tolerance induction and its effects on associated regulatory cellular populations prior to disease initiation. Our experiments demonstrate that Opn drives protective antigenic tolerance by inducing accumulation of IFN-β–producing plasmacytoid dendritic cells, as well as regulatory T cells, in mediastinal lymph nodes. We also show that, in the absence of TLR triggers, recombinant Opn, and particularly its SLAYGLR motif, directly induces IFN-β expression in Ag-primed plasmacytoid dendritic cells, which renders them extra protective against induction of allergic airway disease upon transfer into recipient mice. Lastly, we show that blockade of type I IFNR prevents antigenic tolerance induction against experimental allergic asthma. Overall, we unveil a new role for Opn in setting up a tolerogenic milieu boosting antigenic tolerance induction, thus leading to prevention of allergic airway inflammation. Our results provide insight for the future design of immunotherapies against allergic asthma. ***The Journal of Immunology*****, 2018, 200: 000–000.**

Mechanisms of central and peripheral tolerance are crucial for maintaining immune system homeostasis and preventing exaggerated immune responses to intrinsically harmless self- or foreign Ags. Failure of this mechanism could lead to the development of chronic inflammation, such as allergic asthma and autoimmune diseases.

Because the incidence of allergic disease has risen dramatically, much effort has been put into determining the control mechanisms of peripheral tolerance to allergens in an attempt to find a treatment or prevention strategy for allergic disease. Allergic asthma is a disease caused by aberrant T_H2 immune responses to inhaled allergens leading to eosinophilic airway inflammation, mucus hypersecretion, and variable airway obstruction (1). Regulatory T (Treg) cells are important suppressors of dysregulated T_H2 responses to inhaled Ags, because constitutive or induced deficiency of these cells leads to severe asthmatic reactions (2, 3). Likewise, several groups have demonstrated that conventional dendritic cells (cDCs) and plasmacytoid dendritic cells (pDCs) are key regulators of T_H2 responses in allergic airway inflammation (4–7). As in many processes of immunoregulation, cytokines like TGF-β1 and IL-10 are also important regulators of tolerance to inhaled Ags (3, 8, 9).

Osteopontin (Opn) is a cytokine expressed by immune cells, such as activated T cells and dendritic cells (DCs), as well as by nonimmune cells, including tumor cells and stromal cells (10–12). In inflammatory conditions, Opn affects DC function (5, 13–18) and can drive T_H1, T_H2, and T_H17 effector immune responses (5, 11, 13, 14, 19, 20). In contrast, Opn is constitutively expressed by a great variety of cells under noninflammatory conditions (12, 21–23), but its physiological significance is largely unknown. For example, secreted Opn (sOpn) is expressed in the bone marrow (BM) and also upon inflammatory conditions, primarily in the form of thrombin-cleaved fragments (24, 25). Opn fragments have binding motifs for several integrins: the SLAYGLR motif specifically interacts with integrins α4β1, α9β1, and α4β7, whereas the RGD motif interacts with the αvβ3, αvβ5, αvβ1, and α5β1 integrins (12, 26). In addition, the C-terminal half of Opn interacts with certain CD44 variants (12, 27). Thrombin cleavage of Opn reveals the otherwise cryptic SLAYGLR domain, and this modification is vital for its interaction with α9β1 integrin (28).

*Cellular Immunology Laboratory, Center for Basic Research, Biomedical Research Foundation of the Academy of Athens, 11527 Athens, Greece; †VIB Center for Inflammation Research, Ghent University, 9052 Ghent, Belgium; ‡Institute of Infection Immunology, TWINCORE, Centre for Experimental and Clinical Infection Research, 30625 Hannover, Germany, a Joint Venture between the Helmholtz Centre for Infection Research, 38124 Braunschweig, Germany and the Hannover Medical School, 30625 Hannover, Germany; and §Bioceros BV, 3584 CM Utrecht, the Netherlands

[1]T.A., E.K., and D.C.M.S. contributed equally to this work.

ORCIDs: 0000-0002-4002-6008 (T.A.); 0000-0002-2299-1007 (E.K.); 0000-0001-6278-4144 (N.P.); 0000-0002-1569-1508 (V.P.).

Received for publication September 22, 2017. Accepted for publication December 4, 2017.

This work was supported by the European Research Council (ERC) under the European Union's Seventh Framework Program (FP/2007-2013)/ERC Grant Agreement 243322 (to V.P.) and by an Odysseus grant from the Flemish government (to B.N.L.). T.A. is the recipient of a European Respiratory Society fellowship and a European Academy of Allergy and Clinical Immunology fellowship.

T.A., B.N.L., and V.P. designed the research; T.A., E.K., D.C.M.S., M.A., N.P., and H.H. performed experiments; L.B. and T.S. contributed new reagents; T.A., E.K., D.C.M.S., and V.P. analyzed data; T.A., E.K., B.N.L., and V.P. wrote the manuscript; and B.N.L. and V.P. supervised the study.

Address correspondence and reprint requests to Dr. Vily Panoutsakopoulou, Biomedical Research Foundation of the Academy of Athens, 4 Soranou Efessiou Street, 11527 Athens, Greece. E-mail address: vpan@bioacademy.gr

The online version of this article contains supplemental material.

Abbreviations used in this article: AHR, airway hyperresponsiveness; B6, C57BL/6J; BAL, bronchoalveolar lavage; BDCA2, pDC-specific type II C-type lectin; BM, bone marrow; cDC, conventional dendritic cell; DC, dendritic cell; DEREG, depletion of Treg cell; Derp1, *Dermatophagoides pteronyssinus* allergen 1; dLN, draining lymph node; DT, diphtheria toxin; DTR, diphtheria toxin receptor; frOpn, $Opn_{134–153}$ fragment; i.n., intranasal(ly); LN, lymph node; MFI, mean fluorescence intensity; mLN, mediastinal LN; MOG, myelin oligodendrocyte glycoprotein; Opn, osteopontin; PAS, periodic acid–Schiff; pDC, plasmacytoid dendritic cell; Penh, enhanced pause; rOpn, recombinant Opn protein; sOpn, secreted Opn; Spp1, secreted phosphoprotein 1; Tg, transgenic; Treg, regulatory T.

Copyright © 2018 by The American Association of Immunologists, Inc. 0022-1767/18/$35.00

Downloaded from http://www.jimmunol.org/ by guest on January 17, 2018

Recent reports show that Opn is expressed in Foxp3$^+$ Treg cells (29, 30), suggesting its possible role in immune regulation. In this study, we test whether Opn affects tolerance induction during intranasal (i.n.) administration of endotoxin-free Ag. Our results unveil a novel role for Opn as a tolerance enhancer against allergic airway disease, setting up an immunoregulatory milieu and potentiating CCR7-expressing pDC recruitment to the draining lymph nodes (dLNs). In addition, we reveal that, in the absence of pathogen-associated molecular patterns, sOpn, and specifically its integrin-binding SLAYGLR motif, induces low levels of IFN-β expression in Ag-primed pDCs. SLAYGLR-treated pDCs are highly efficient at suppressing allergic airway inflammation via type I IFN. Finally, we show that type I IFNs are crucial during antigenic tolerance induction against allergic airway disease.

Materials and Methods

Mice

BALB/c, C57BL/6J (B6), OVA-specific TCR-transgenic (Tg) C.Cg-Tg (DO11.10)10Dlo/J (DO11.10), C.129P2(B6)-IL-10^{tm1Cgn}/J, B6(Cg)-Il10$^{tm1.1Karp}$ (*Il10*^{GFP}), B6.129-*Ifnb1*^{tm1Lky}/J (*Ifnb*^{EYFP}), B6.129S2-

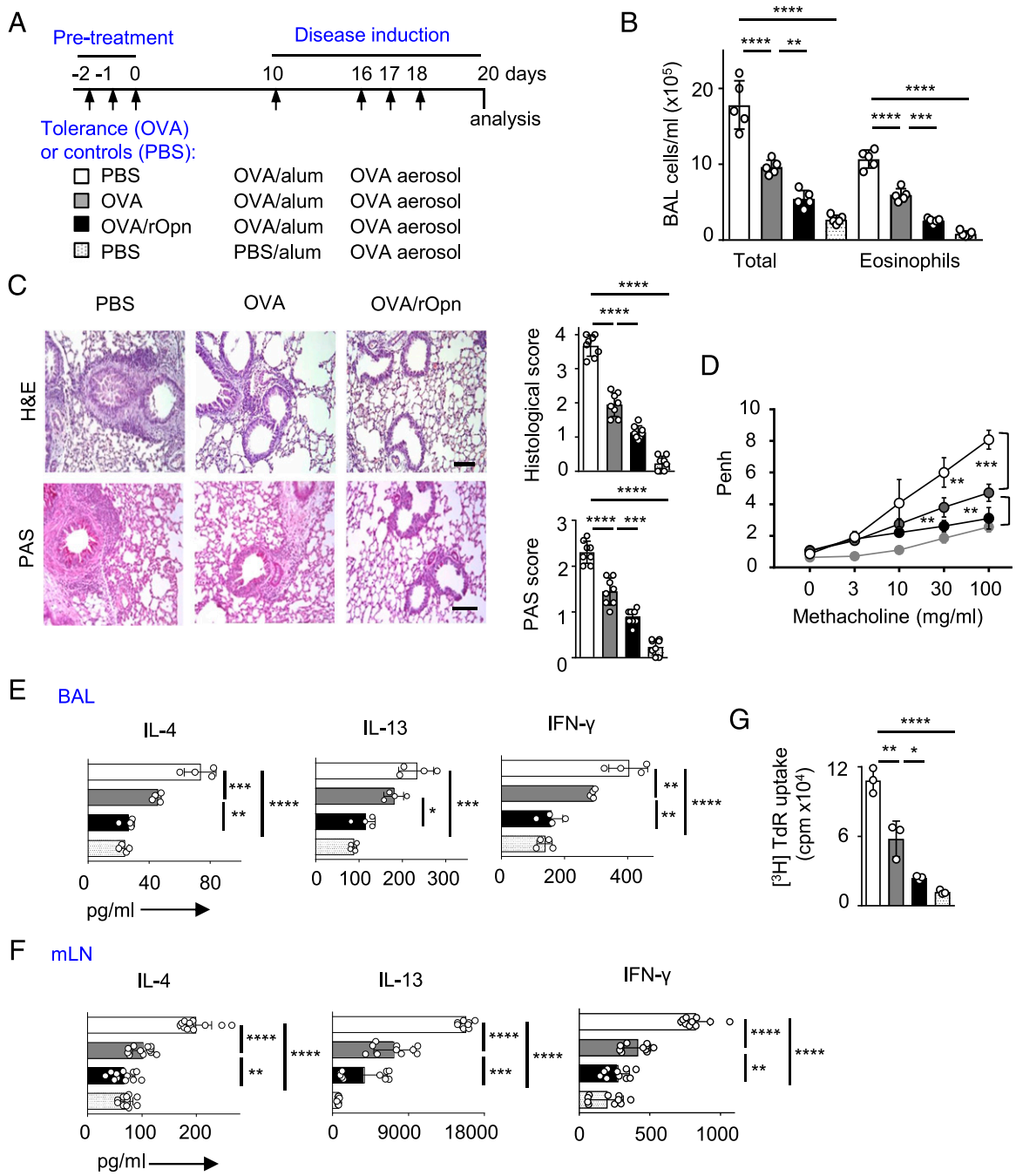

FIGURE 1. Opn administration boosts antigenic tolerance, leading to increased protection from allergic airway disease. (**A**) Experimental protocol used for endotoxin free-tolerance (OVA administration) induction, followed by allergic asthma induction. Controls were mice pretreated with PBS (no tolerance) and subsequent allergic airway disease induction (white bars). Controls for allergic airway disease were mice pretreated and sensitized with PBS. (**B**) Total cell counts (in BAL) and eosinophils. (**C**) Representative photomicrographs of H&E- and PAS-stained lung sections and histological scores. Scale bars, 100 μm. (**D**) AHR (depicted as Penh) on day 19. Levels of IL-4, IL-13, and IFN-γ in BAL (**E**) and in the supernatant of mLN cells (**F**) stimulated ex vivo with OVA. (**G**) [^{3}H]Thymidine incorporation of mLN cells stimulated ex vivo with OVA. The same numbers of pooled mLN cells were cultured in 3, 4, 10, or 12 different wells per group in (E)–(G). Data are mean ± SEM (n = 8 mice per group), one representative of three independent experiments. *$p \leq 0.0332$, **$p \leq 0.0021$, ***$p \leq 0.0002$, ****$p < 0.0001$.

Downloaded from http://www.jimmunol.org/ by guest on January 17, 2018

Ifnar1^{tm1Agt}/Mmjax (*Ifnar1*$^{-/-}$), and B6-Tg (C-type lectin domain family 4, member C [CLEC4C]–heparin binding EGF like growth factor [HBEGF]) 956Cln/J (pDC-specific type II C-type lectin [BDCA2]-diphtheria toxin receptor–[DTR]) mice were purchased from The Jackson Laboratory (Bar Harbor, ME). B6-Tg Foxp3-DTR/EGFP (depletion of Treg cell [DEREG]) mice were provided by T.S. B6.129S6(Cg)-secreted phosphoprotein 1 (Spp1)^{tm1Blh}/J (*Spp1*$^{-/-}$) mice were kindly provided by Dr. L. Liaw (Maine Medical Center Research Institute, Scarborough ME). All mice used in this study were 8–10-wk-old females. Mice were housed at the Animal Facility of the Biomedical Research Foundation of the Academy of Athens and at the University Hospital Ghent (Ghent, Belgium). Use of mice in this study was reviewed and approved by the Bioethics Committee of the Biomedical Research Foundation of the Academy of Athens, the Veterinarian Office of Attica, and the Animal Ethics Committee of Ghent University. All procedures were in accordance with the National Institutes of Health Statement of Compliance (Assurance) with Standards for Humane Care and Use of Laboratory Animals (A5736–01) and with the European Union Directive 86/609/EEC for the protection of animals used for experimental purposes.

In vivo experimental protocols

For tolerance induction, mice received 200 μg of EndoGrade OVA (Hyglos) i.n. in the presence of 2.5 μg recombinant Opn protein (rOpn) (R&D Systems), 72 ng of synthetic secreted $Opn_{134–153}$ fragments (frOpn; IVPTVDVPNGRGDSLAYGLR), or PBS (control). The RGD domain (Arg-Gly-Asp) of frOpn1 is scrambled to RAA (Arg-Ala-Ala). The SLAYGLR domain (Ser-Leu-Ala-Tyr-Gly-Leu-Arg) of frOpn2 is scrambled to LRAGLRS (Leu-Arg-Ala-Gly-Leu-Arg-Ser). frOpn3 has the RGD and SLAYGLR domains scrambled to RAA and LRAGLRS, respectively (Caslo Laboratory ApS). Opn oligopeptide fragments have been described previously (31). Myelin oligodendrocyte glycoprotein $(MOG)_{35–55}$ peptide (MEVGWYRSPFSRVVHLYRNGK; Caslo Laboratory ApS) was also used for tolerance induction (250 μg per mouse i.n.). Mice were euthanized 36–40 h later and analyzed. In certain experiments, tolerance was induced prior to allergic airway disease induction: mice received 200 μg of EndoGrade OVA (i.n.) on days −2, −1, and 0 in the presence of 2.5 μg of rOpn or 72 ng of frOpn1-3 synthetic fragments (i.n.). Control mice received PBS. Allergic airway disease (asthma) was subsequently induced: on day 10, mice were immunized with chicken OVA Grade V (Sigma-Aldrich; 50 μg) in 0.2 ml of aluminum hydroxide (alum) (Serva), followed by three challenges with 5% aerosolized

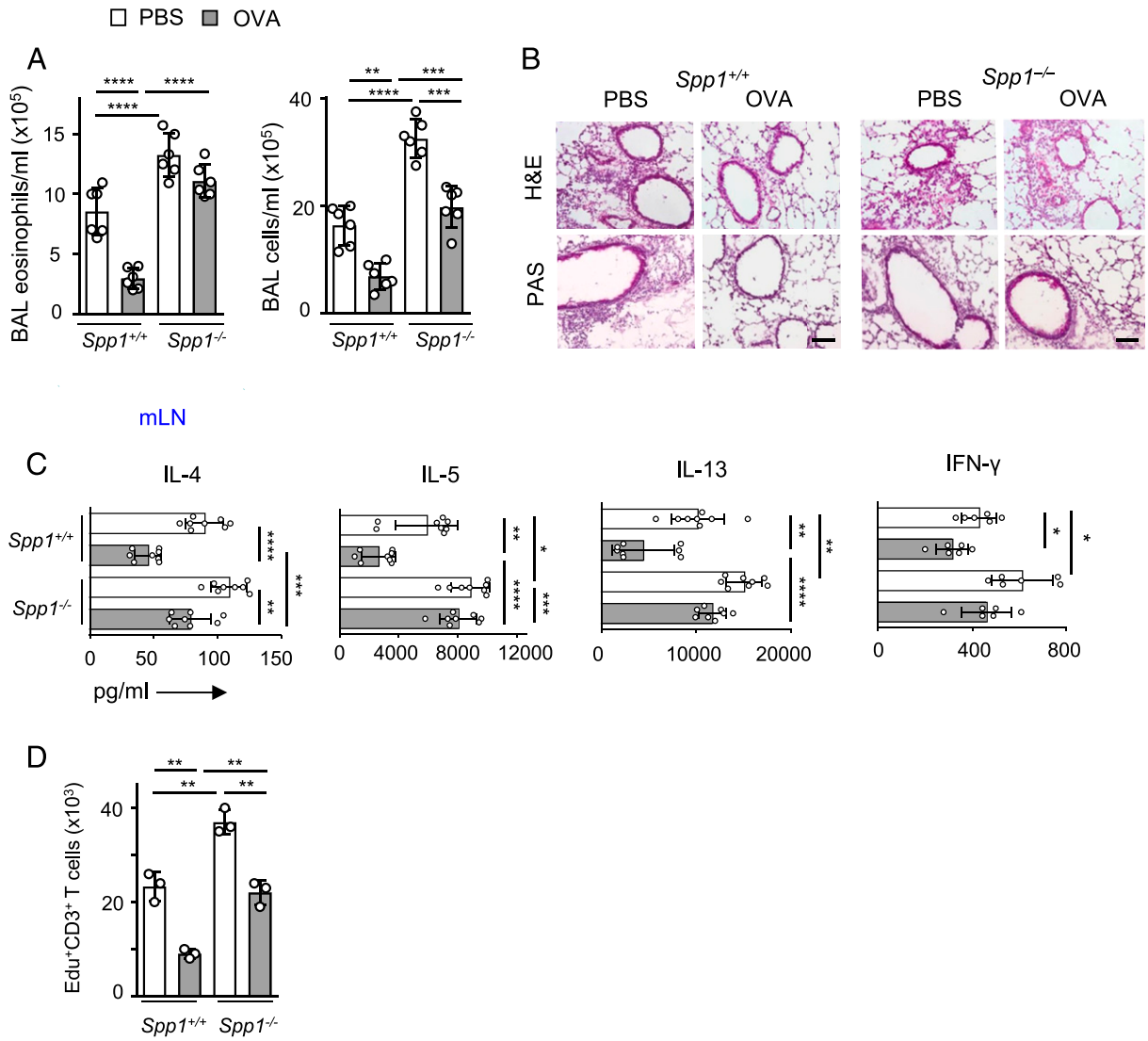

FIGURE 2. *Spp1*$^{-/-}$ mice are more resistant to tolerance induction. *Spp1*$^{-/-}$ or *Spp1*$^{+/+}$ mice received three doses of endotoxin-free OVA or PBS i.n. on days −2, −1, and 0 (as in Fig. 1A). On day 10, mice were sensitized i.p. with OVA in alum and were subsequently challenged through the airways with aerosolized OVA between days 16 and 18. Analysis was performed on day 20. (**A**) Differential eosinophil and total cell counts in BAL. (**B**) Lung inflammation in H&E-stained sections and mucus secretion in PAS-stained sections from PBS- and OVA-treated *Spp1*$^{+/+}$ and *Spp1*$^{-/-}$ mice. Scale bar, 100 μm. Levels of IL-4, IL-5, IL-13, and IFN-γ in supernatants of OVA-stimulated dLN cells (**C**) and percentages of Edu^{+}CD3^{+}CD4^{+} T cells in OVA-stimulated dLN cells (**D**) in both mice groups. The same numbers of pooled mLN cells were cultured in three, six, or eight different wells per group in (C) and (D). Data are mean ± SEM ($n = 6$ mice per group), one representative of three independent experiments. *$p \leq 0.0332$, **$p \leq 0.0021$, ***$p \leq 0.0002$, ****$p < 0.0001$.

Downloaded from http://www.jimmunol.org/ by guest on January 17, 2018

OVA between days 16 and 18, as described (5, 15). Mice were euthanized 2 d after the last aerosol treatment (on day 20). DEREG mice received 1 μg of diphtheria toxin (DT; Sigma-Aldrich) (32) or PBS i.p. on days −3 and −2 (6 h prior to i.n. OVA administration). For the DT control group, non-Tg littermates were administered DT. For pDC depletion, mice received 225 μg of 120G8 pDC-depleting Ab (IgG2a; Dendritics, Lyon, France) (33) or an IgG2a isotype control Ab i.p. on days −6, −5, −4, and −3. As in Fig. 4A, mice received 200 μg of EndoGrade OVA i.n., along with 2.5 μg of rOpn, on days −2, −1 and 0 and were euthanized 7 d later. For pDC depletion in *BDCA2-DTR* mice, 120 ng of DT was administered i.p. on days −4 and −3 in the 7-d tolerance-induction protocol (as in Fig. 4A) (34). Efficient pDC depletion (≥95%) from dLNs in both approaches was determined by FACS analysis (data not shown). For neutralization of IFNAR1, mice received 20 μg of a polyclonal affinity-purified neutralizing Ab to mouse IFNAR1 (clone MAR1-5A3; eBioscience) or goat IgG isotype control (R&D Systems) i.p. 2 h before tolerance induction. For allergy induction, after IFNAR1 neutralization and tolerance, mice were immunized with chicken OVA on day 15, and OVA challenges were performed between days 21 and 23.

Enhanced pause

Lung function was measured in mice 24 h after the final OVA challenge (day 19) by whole body plethysmography (Buxco Technologies) to calculate enhanced pause (Penh). Responses to inhaled methacholine (Sigma-Aldrich) at concentrations of 3–100 mg/ml were measured for 1 min, as previously described (5).

Analysis of bronchoalveolar lavage and lung histology

Bronchoalveolar lavage (BAL) harvesting and analysis were performed as previously described (35, 32). For histological analysis, paraffin-embedded (4-μm) lung sections were stained with H&E and quantified as previously described (35). Goblet cells were quantified in Periodic acid–Schiff (PAS)-stained lung sections (5). A semiquantitative scoring system was used to grade the area of lung infiltrated, as previously described (36). Goblet cells were counted on PAS-stained sections using an arbitrary scoring system, as previously described (36).

pDC generation from BM, cultures, and adoptive transfer

For pDC generation, BM cells were isolated and cultured with recombinant human Flt3 ligand, as described (37). On day 11, 7AAD$^-$ CD3$^-$CD19$^-$CD11c$^+$B220$^+$PDCA1$^+$Siglec-H$^+$ pDCs were sorted to ≥98% purity using a FACSAria III, after enrichment with a CD11c MicroBeads Kit (Miltenyi Biotec). Sorted pDCs from BM cultures were conditioned for 16 h with 100 μg/ml EndoGrade OVA or LoTox *Dermatophagoides pteronyssinus* allergen 1 (Derp1; Indoor Biotechnologies) in the presence of 250 ng/ml rOpn, 18.2 ng/ml frOpn1 or frOpn3, or PBS. After the culture with OVA, pDCs were washed and analyzed or transferred i.v. via the tail vein (10^6 cells per mouse). Allergic asthma

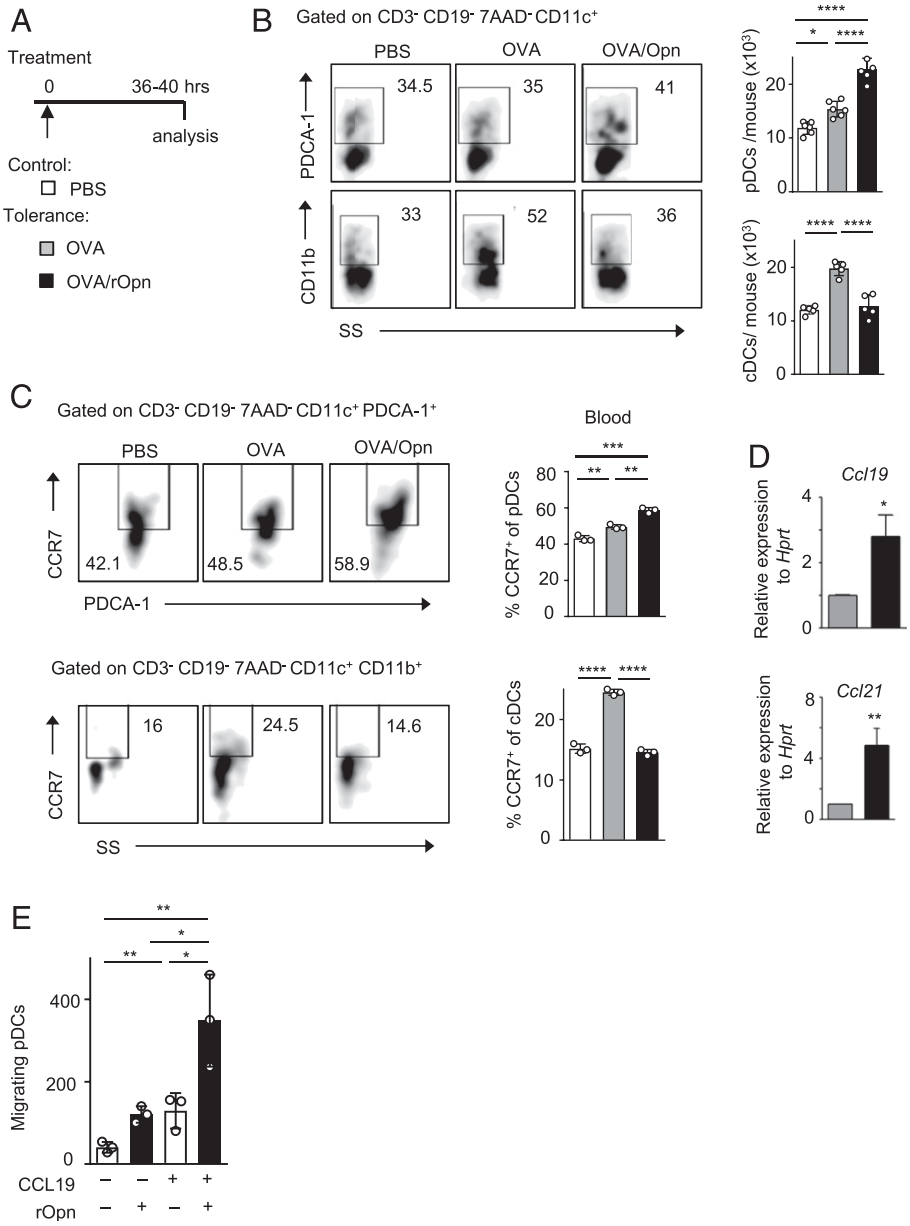

FIGURE 3. Opn-induced accumulation of pDCs in dLN and differential CCR7 expression. (**A**) Treatment of mice with endotoxin-free OVA alone or together with endotoxin-free rOpn (tolerance induction), or treatment of mice with PBS without OVA for control. (**B–D**) Controls (without tolerance) were PBS-treated mice (white bars). 7AAD$^-$ CD3$^-$CD19$^-$CD11c$^+$PDCA-1$^+$CCR7$^+$ pDCs and 7AAD$^-$CD3$^-$CD19$^-$CD11c$^+$CD11b$^+$ CCR7$^+$ cDCs quantified in dLNs by flow cytometry. (B) Representative percentages in flow cytometric plots and numbers of dLN pDCs (upper panels) and cDCs (lower panels). (C) Representative flow cytometric plots and percentages of peripheral blood CCR7$^+$ pDCs and cDCs among total pDCs and cDCs, respectively. (D) Relative expression to *Hprt* of *Ccl19* and *Ccl21* in dLNs of tolerized mice. Data are mean ± SEM (n = 10 mice per group; cDNAs were pooled from three separate experiments). (**E**) Sorted pDCs from LNs and spleens of naive BALB/c mice were pulsed with vehicle or rOpn for 24 h and then subjected to transmigrate in response to CCL19. Numbers of migrating PBS-treated pDCs (white bars) or rOpn- treated pDCs (black bars). Triplicate wells of pooled pDCs sorted from spleens and LNs (n = 8). Data are mean ± SEM (n = 5–8 mice per group), one representative of five independent experiments (A–C) and from three independent experiments (E). *$p \leq 0.0332$, **$p \leq 0.0021$, ***$p \leq 0.0002$, ****$p < 0.0001$.

Downloaded from http://www.jimmunol.org/ by guest on January 17, 2018

was induced in mice 7 d later. Mice were euthanized 2 d after the last OVA challenge (Figs. 7B, 10A).

Cell culture, proliferation, and cytokine analysis

Isolated dLN cells (2×10^5–10^6) were cultured with 125 μg/ml OVA (Sigma-Aldrich) for 48 h. We performed proliferation assays with thymidine incorporation, as previously described (38). For certain experiments, proliferation of cells was measured as the percentage of Edu^+ cells by FACS, using a Molecular Probes kit. For cytokine measurements, we used ELISA kits for IL-5 and IFN-γ (both from BD Biosciences), IL-4 and IL-13 (both from R&D Systems), and IFN-β (BioLegend).

Flow cytometry

Freshly isolated live ($7AAD^-$; BD Biosciences) dLN cells and in vitro–derived BM cells were stained with combinations of fluorochrome-conjugated Abs to CD4–Pacific Blue or CD4-PE/Cy5 (clone GK 1.5); CD3-PE/Cy7, CD3-PE/Cy5, CD3-PE, or CD3-FITC (17A2); CD11c-PE/Cy7, CD11c-FITC, or CD11c-Orange 605 (N418); CD11b-PE/Cy7 or CD11b-FITC (M1/70); B220-PE or B220-BV 510 (RA3-6B2); CCR7-PE (4B12); Siglec-H–Pacific Blue or Siglec-H–FITC (551); PDCA-1–PE or PDCA-1–FITC (927); CD19-PE/Cy7 or CD19-PE/Cy5 (6D5); CD25-PE (PC61.5) (BioLegend); and T1ST2 (DIH9) (T1ST2-FITC [MD Biosciences] or T1ST2–PE [BioLegend]). For intranuclear staining of Foxp3, a permeabilization kit and Abs (Foxp3–Pacific Blue or Foxp3-PE/CyC5; clone FJK-16s) were used (eBioscience). Flow cytometric measurements were performed using an Attune Acoustic Focusing Cytometer (Applied Biosystems) and a FACSAria III (BD). FACS sorting of pDCs was performed using a FACSAria III. Data analysis was performed with FlowJo software (TreeStar).

Chemotaxis assay

Sorted pDCs from lymph nodes (LNs) and spleen of BALB/c mice were treated with rOpn (500 ng/ml) for 18–20 h and assayed for migration in response to chemokine CCL19 or CCL21 (200 ng/ml) (R&D Systems). The lower chambers of Transwell plates (QCM Chemotaxis Cell Migration Assay, 24-well [5 μm], colorimetric; Millipore) were filled with 500 μl of serum-free medium in the presence or absence of chemokines. DCs (10^5 cells per 200 μl) resuspended in serum-free medium were deposited in the upper chambers of the Transwell plates and allowed to migrate for 4 h at 37°C in 5% CO_2. For each experiment, pooled total cells from spleen and inguinal and mesenteric LNs of mice ($n = 8$) were used, and pDCs were isolated by sorting.

Suppression assay and Treg cell induction in vitro

BM-derived pDCs, pretreated or not with OVA and/or rOpn, were cultured with naive DO11.10 $CD4^+$ T cells for 3 d at a 1:5 ratio. T cells were harvested and cultured in the presence of 1 ng/ml recombinant mouse IL-2 (R&D Systems) for an additional 7 d. Suppressive activity was assayed on 10^5 freshly purified CFSE (Invitrogen)-labeled DO11.10 $CD4^+$ T cells stimulated with 10^4 irradiated BALB/c splenocytes, with 1 μg/ml $OVA_{323–339}$ peptide (Caslo Laboratory ApS), in the presence or absence of 10^5 DC-stimulated T cells. CFSE uptake was assayed 7 d later (Fig. 7A).

Quantitative real-time PCR analysis

Total RNA was extracted from cells isolated from dLNs with anti–mPDCA-1 and CD11c MicroBeads (Miltenyi Biotec) and further purified with FACS sorting. cDNA synthesis was performed as described (31). Primers were designed using the Primer3 program and are shown in Supplemental Table I (MWG Eurofins). *Hprt*, *Foxp3*, *Il-10*, *Il27p28*, and *Spp1* primers were described previously (31). Real-time PCR was performed and analyzed as previously described (31). The reference gene used for real-time PCR analysis was *Hprt*.

Statistical analysis

Data were analyzed using Prism 7 software (GraphPad). The two-tailed Student *t* test was used for statistical analyses of two-group comparisons. Multigroup comparisons were performed using two-way ANOVA, followed by the Bonferroni correction for the multiplicity of tests. All results are presented as mean ± SEM. In all experiments, statistical significance was defined as $*p \leq 0.0332$, $**p \leq 0.0021$, $***p \leq 0.0002$, and $****p < 0.0001$.

Results

Opn boosts antigenic tolerance leading to increased protection from allergic airway disease

To address whether Opn plays a role in tolerance induction, mice received endotoxin-free chicken OVA, together with endotoxin-free rOpn or PBS control i.n., and protection against disease was assessed using a well-established model of allergic asthma (39) (Fig. 1A). OVA-tolerized mice showed a significant decrease in BAL total cells and eosinophils, as well as lung tissue inflammatory scores and mucus secretion (Fig. 1B, 1C), compared with nontolerized mice. In addition, Penh in OVA-tolerized mice was significantly reduced (Fig. 1D). Importantly, in OVA/rOpn-tolerized mice, numbers of eosinophils in BAL (Fig. 1B), airway hyperresponsiveness (AHR) (Fig. 1D), lung leukocytic infiltration, and mucus secretion (Fig. 1C) were further reduced compared with OVA-tolerized mice. Furthermore, OVA/rOpn tolerization resulted in significantly reduced levels of IL-4, IL-13, and IFN-γ in BAL, as well as a reduction in OVA-specific responses in mediastinal lymph node (mLN) cell cultures and in T_H cell proliferation, compared with OVA tolerization (Fig. 1E–G). Studies from our group (5, 15) and other investigators (40–42) have shown that there are high levels of IFN-γ production in allergic airway disease. The above findings indicated that administration of Opn, along with OVA, promotes enhanced tolerance, conferring significant protection from disease development.

We next investigated whether Opn deficiency had any effect on tolerance induction. Tolerance induction in $Spp1^{-/-}$ mice was not as effective as in $Spp1^{+/+}$ mice, because we did not note a significant

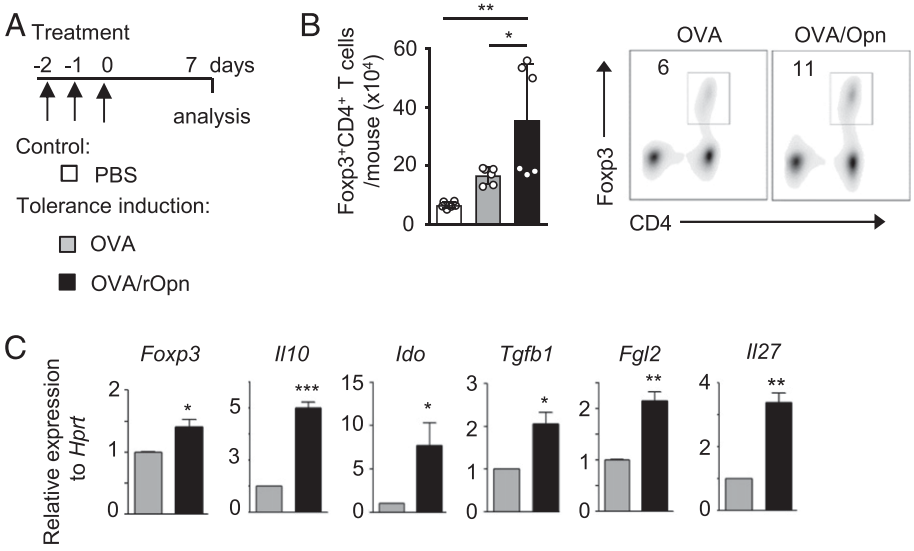

FIGURE 4. Opn administration with Ag promotes accumulation of Treg cells and immunoregulatory gene expression in dLNs. (**A**) Mice received three doses of endotoxin-free OVA for tolerance induction, along with rOpn or PBS. Controls (without tolerance) were PBS-treated mice (white bars). (**B**) Percentages and numbers of $CD3^+CD4^+Foxp3^+$ T cells quantified in dLNs by flow cytometry at day 7. (**C**) Relative expression to *Hprt* of immunoregulatory genes in dLNs. cDNAs were pooled from three separate experiments. Data are mean ± SEM ($n = 6$ mice per group), one representative of three independent experiments. $*p \leq 0.0332$, $**p \leq 0.0021$, $***p \leq 0.0002$.

Downloaded from http://www.jimmunol.org/ by guest on January 17, 2018

change in the number of eosinophils or total cell numbers in BAL (Fig. 2A). In accordance, tolerogenic i.n. OVA administration in *Spp1*$^{-/-}$ mice could not efficiently dampen the inflammation and mucus secretion in the lung, whereas it was very efficient in *Spp1*$^{+/+}$ mice (Fig. 2B). T_H2 cytokine production by OVA–stimulated mLN cells was also lower in OVA-tolerized *Spp1*$^{-/-}$ mice compared with PBS-treated *Spp1*$^{-/-}$ mice (Fig. 2C). OVA-stimulated mLN cells from OVA-tolerized *Spp1*$^{+/+}$ mice produced ~50% lower levels of T_H2 cytokines compared with cells from PBS-treated *Spp1*$^{+/+}$ mice, whereas OVA-tolerized *Spp1*$^{-/-}$ mice had a smaller reduction in cytokine levels compared with *Spp1*$^{+/+}$ mice (Fig. 2C). The reduction in IFN-γ levels was similar among groups (Fig. 2C). Finally, OVA tolerization of *Spp1*$^{-/-}$ mice resulted in a smaller decrease in the percentages of CD3$^+$ T proliferating cells in cultures of mLN cells compared with those from *Spp1*$^{+/+}$ OVA-treated mice (Fig. 2D). The above results strongly support that tolerance induction is more effective in the presence of Opn.

Opn administration along with Ag increases accumulation of tolerogenic pDCs

Migratory nonlymphoid tissue DCs transporting Ags to LNs are involved in promoting tolerance to self-antigens in the steady-state. Because pDCs constitute a tolerogenic DC subset (43–47), and Opn has a dual role in the recruitment of DC subsets (5), we analyzed pDC numbers in dLNs of OVA-tolerized mice and PBS-treated controls (Fig. 3A). Numbers of dLN pDCs were increased in the OVA-treated group compared with the PBS control group (Fig. 3B). Mice treated with OVA/rOpn had increased percentages and significantly higher total numbers of pDCs in the dLNs at 36–40 h following treatment compared with OVA treatment (Fig. 3B). In contrast, cDC numbers in the dLNs of OVA/rOpn mice were significantly reduced and percentages were lower compared with OVA treatment alone (Fig. 3B). Therefore, administration of Opn during tolerance induction affects the balance of DC subsets in dLNs by increasing the numbers of pDCs and reducing the numbers of cDCs.

The importance of Opn for DC subset recruitment in tolerance was also demonstrated using Opn-deficient mice. Antigenic tolerance induction in *Spp1*$^{-/-}$ mice resulted in a significant reduction in pDC numbers in their dLNs compared with *Spp1*$^{+/+}$ mice (Supplemental Fig. 1). At the same time, cDC numbers were significantly increased in dLNs of *Spp1*$^{-/-}$ mice (Supplemental Fig. 1). Conclusively, these results show that tolerogenic administration of OVA in an Opn-efficient microenvironment enhances pDC accumulation in dLNs.

Administration of Opn during tolerance induction regulates CCR7 expression affecting DC subset homing to dLNs

To explore the reason for the increased numbers of pDCs in dLNs of Opn-treated mice, we investigated the effect of Opn on CCR7$^+$ pDCs. CCR7 is a chemokine receptor responsible for homing of DCs to dLNs (48–50). We quantified CCR7$^+$ DC subsets in peripheral blood 36 h following OVA/rOpn tolerogenic administration (Fig. 3A). The percentages of CCR7$^+$ pDCs per total pDC numbers were significantly elevated in the peripheral blood of mice treated with rOpn during tolerance induction compared with PBS-treated mice (Fig. 3C). The percentages of CCR7$^+$ cDCs per total cDC numbers originating from the peripheral blood of mice that had been administered OVA/rOpn were significantly decreased compared with OVA-administered mice (Fig. 3C). Our results demonstrate that Opn leads to enhanced migratory CCR7$^+$ pDC percentages per total pDCs in the blood.

We also found that OVA/rOpn-administered mice had significantly higher levels of *Ccl19* and *Ccl21* (encoding CCL19 and CCL21 chemokines that bind to CCR7) expression in their dLNs compared with OVA-administered mice (Fig. 3D), possibly attracting the increased numbers of CCR7$^+$ pDCs to dLNs. Indeed, in vitro transmigration assays showed that sorted pDCs from naive mice pretreated with rOpn had a 2-fold increase in CCL19-induced chemotaxis compared with PBS-treated pDCs (Fig. 3E). The above findings demonstrate that, during tolerance induction, Opn can differentially regulate the percentages of CCR7$^+$ DC subsets, thereby affecting their chemotactic migration to dLNs in favor of pDCs. Moreover, the observed increased gene expression of the CCR7 ligands CCL19 and CCL21 provide an extra explanation for the rOpn-mediated migration of pDCs to dLNs.

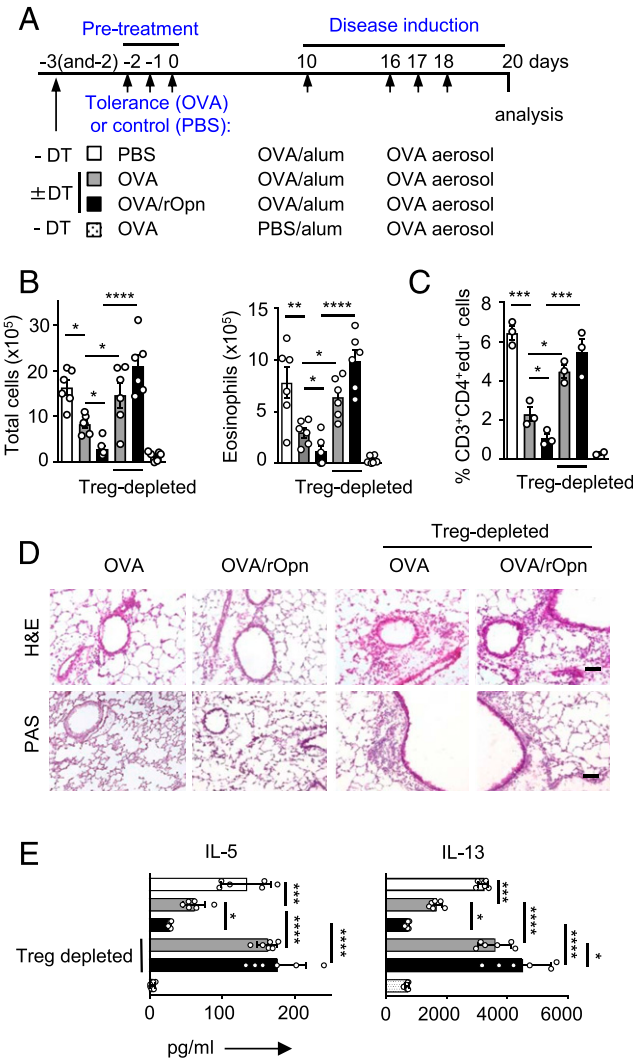

FIGURE 5. Opn-induced tolerance is Treg cell dependent. (**A**) Tolerance induction in DT-treated DEREG and control DEREG mice without DT injections. Controls (without tolerance) were DEREG mice pretreated with PBS, with subsequent allergy induction (white bars). (**B**) Eosinophil and total cell counts in BAL. (**C**) Numbers of Edu$^+$CD3$^+$CD4$^+$ T cells per 25 × 10^4 OVA-stimulated dLN cells. (**D**) Lung inflammation and mucus secretion in H&E-stained (upper panels) and PAS-stained (lower panels) slides. Scale bars, 100 μm. (**E**) Levels of IL-5 and IL-13 in supernatants of OVA-stimulated dLN cells. The same numbers of pooled mLN cells were cultured in three (C) or six (D) different wells per group. Data are mean ± SEM (n = 6 mice per group), one representative of three independent experiments. *$p \leq 0.0332$, **$p \leq 0.0021$, ***$p \leq 0.0002$, ****$p < 0.0001$.

Downloaded from http://www.jimmunol.org/ by guest on January 17, 2018

Opn enhances pDC-dependent Foxp3$^+$ Treg cell accumulation and promotes an immunoregulatory milieu in dLNs

Because Ag administration for tolerance induction leads to generation of Treg cells (51), we investigated whether Opn had an effect early on this process. We administered OVA with rOpn (OVA/rOpn) or PBS i.n. to mice for three consecutive days, and mice were analyzed 1 wk later (Fig. 4A). OVA/rOpn-treated mice showed a nearly 2-fold increase in the percentages, as well as in the total numbers, of CD4$^+$Foxp3$^+$ Treg cells in dLNs compared with OVA-treated mice (Fig. 4B). Increased numbers of Foxp3$^+$ Treg cells in OVA/rOpn-tolerized mice were accompanied by significantly enhanced *Foxp3* expression in dLN cells (Fig. 4C). In addition, OVA/rOpn treatment induced a significant increase in the expression levels of immunoregulatory molecules, such as *Il10*, *Ido*, *Tgfb1*, *Fgl2*, and *Il27*, in dLNs compared with OVA treatment (Fig. 4C). Conclusively, Opn administration, along with Ag, promotes Foxp3$^+$ Treg cell accumulation, resulting in a highly tolerogenic microenvironment in the dLN.

To directly test whether increased numbers of Foxp3$^+$ Treg cells mediate the observed rOpn promotion of tolerance, we depleted Foxp3$^+$ Treg cells prior to tolerance induction using DEREG mice (52) (Fig. 5A). Induction of tolerance with rOpn could not protect Treg-depleted mice, which exhibited increased allergic responses, as demonstrated by increased eosinophilia and lymphocytosis in the BAL, increased T cell proliferation, elevated lung inflammation with enhanced mucus production, and increased OVA-specific cytokine responses compared with Treg-sufficient mice (Fig. 5B–E).

To address whether the Opn-mediated increase in pDC numbers was responsible for the observed accumulation of Foxp3$^+$ Treg cells, we depleted pDCs by administering 120G8 pDC-depleting Ab (33) prior to induction of tolerance and examined the accumulation of Foxp3$^+$ Treg cells in dLNs. This depletion led to a significant reduction in CD4$^+$Foxp3$^+$ Treg cell numbers compared with OVA/rOpn administration in non–pDC-depleted mice (Fig. 6A), resulting in exacerbated allergic airway disease (Fig. 6B). We observed similar effects of rOpn on Treg cellularity in LNs after in vivo depletion of pDCs in *BDCA2-DTR* Tg mice (34) (Supplemental Fig. 2). Thus, Opn-mediated pDC accumulation is responsible, at least in part, for the higher numbers of Treg cells in dLNs. In addition, dLN cells from OVA/rOpn-treated pDC-depleted mice were significantly less capable of suppressing OVA-specific T cell proliferation (Fig. 6C) compared with dLN cells from OVA/rOpn-treated non–pDC-depleted mice, reaching an even lower suppressive ability than that of OVA-treated pDC-depleted dLN cells. Thus, OVA/rOpn treatment

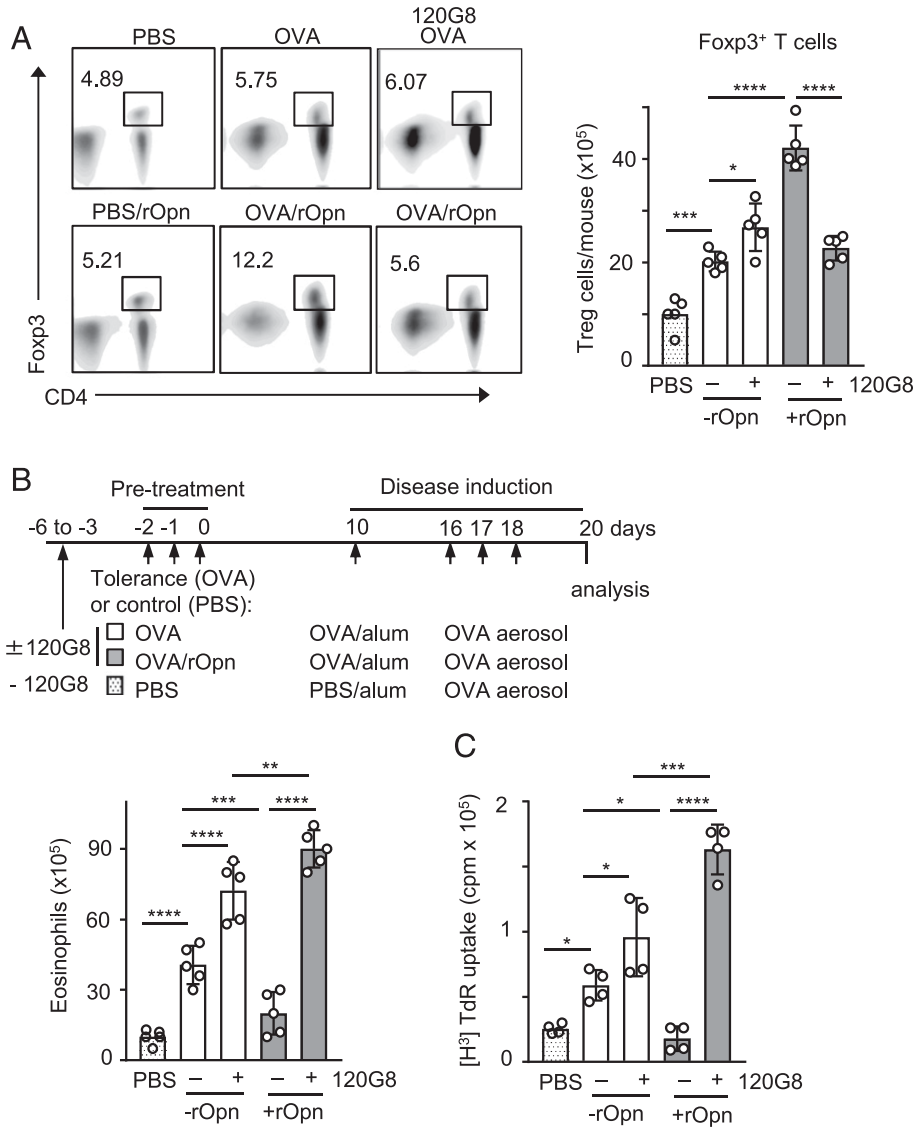

FIGURE 6. Opn-induced tolerance increases pDC numbers, favoring Treg cell accumulation. (**A**) Mice received four doses of 120G8 pDC-depleting Ab or Ig control i.p. on days −6, −5, −4, and −3, followed by tolerance induction for Treg cell generation, with or without rOpn administration. (**B** and **C**) Also, allergic airway disease was subsequently induced on day 10. Control mice were pretreated with PBS (A) or sensitized with PBS (B and C). (A) Representative percentages in flow cytometric plots (left panel) and numbers of Treg cells (CD3$^+$CD4$^+$Foxp3$^+$) accumulated in dLNs (right panel). (B) Eosinophil counts in BAL of allergic mice. (C) [^{3}H]Thymidine incorporation in OVA-stimulated dLN cells. Quadruplicate wells of pooled mLN cells. Data are mean ± SEM (n = 5 mice per group), one representative of three independent experiments. *$p \leq 0.0332$, **$p \leq 0.0021$, ***$p \leq 0.0002$, ****$p < 0.0001$.

Downloaded from http://www.jimmunol.org/ by guest on January 17, 2018

increased the numbers of pDCs, favoring the accumulation of Foxp3$^+$ Treg cells that are crucial for tolerance maintenance.

Opn treatment of pDCs increases their suppressive activity against allergic airway disease

We tested the suppressive function of in vitro OVA/rOpn-treated BM-derived pDCs by coculturing them with CD4$^+$ T cells. T cells obtained from OVA/rOpn-treated pDC cultures significantly suppressed the responses of DO11.10 T cells to OVA compared with T cells obtained from OVA-treated pDC cultures (Fig. 7A).

We also adoptively transferred BM-derived pDCs, which were preconditioned in vitro with OVA or OVA/rOpn, into recipient mice prior to induction of allergic airway inflammation (Fig. 7B).

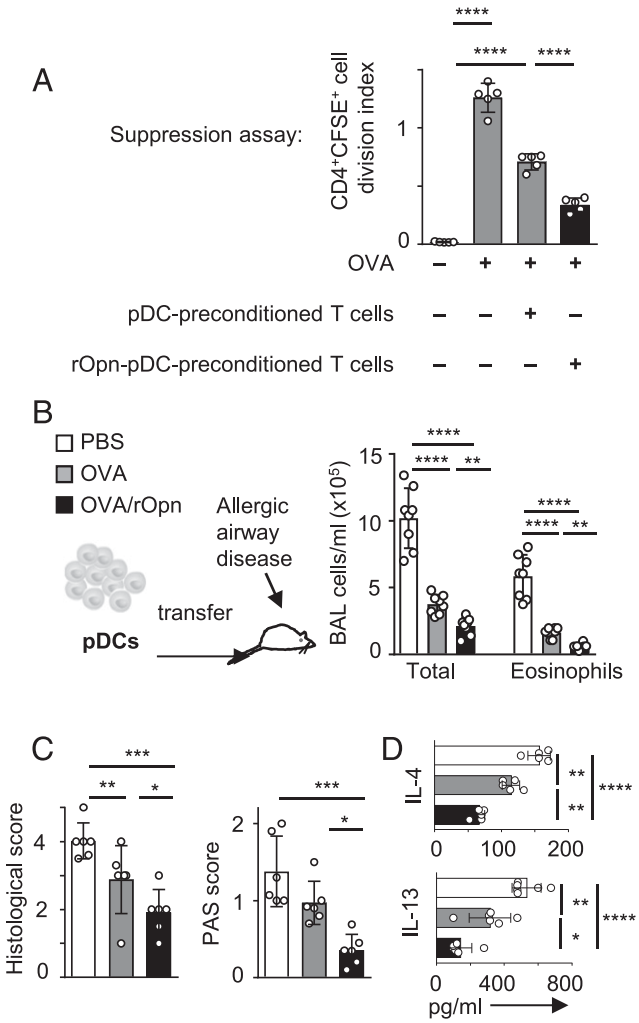

FIGURE 7. rOpn treatment of pDCs increases their suppressive activity against allergic airway disease. (**A**) [^{3}H]Thymidine incorporation in cocultures of DO11.10 T cells preconditioned with $OVA_{323–339}$ and rOpn-treated pDCs with responder DO11.10 T cells. The same numbers of cells were cultured in five different wells per group. Data are mean ± SEM, one representative of three independent experiments. (**B**) Sorted pDCs preconditioned in vitro with PBS or OVA or OVA/rOpn were adoptively transferred to recipient mice before the induction of allergic airway inflammation. Total and eosinophil cell count in BAL were evaluated (day 20). Histological assessment of lung inflammation (H&E scoring) and lung mucus production (PAS score) (**C**) and levels of IL-4 and IL-13 (**D**) in supernatants of OVA-stimulated mLN cells. Different wells of pooled mLN cells. Data are mean ± SEM (n = 6–8 mice per group), one representative of three independent experiments. *$p \leq 0.0332$, **$p \leq 0.0021$, ***$p \leq 0.0002$, ****$p < 0.0001$.

Control mice received PBS-treated pDCs. Total and eosinophil cell numbers, as well as lung tissue inflammatory scores and mucus secretion, were lower in BAL of OVA/rOpn-treated pDC recipient mice compared with OVA-treated pDC recipient mice (Fig. 7B, 7C). Furthermore, OVA/rOpn-treated pDC recipients had significantly reduced OVA-specific responses compared with OVA-treated pDC recipients (Fig. 7D). Thus, OVA/rOpn treatment of pDCs rendered them more regulatory, indicating that Opn affects the intrinsic tolerogenic function of pDCs.

Opn SLAYGLR motif is responsible for pDC recruitment and effective protection from allergic disease

RNA expression analysis revealed that, during tolerance induction, mLN pDCs have increased expression of integrins αvβ3, α4β1, and α9β1 (data not shown). Because the SLAYGLR motif of Opn interacts with α4β1, α4β7, and α9β1 integrins (12), and the RGD motif interacts with the αvβ3 integrin (11, 12), we asked which Opn domain is responsible for the observed effects on pDCs during tolerance induction. Thus, synthetic $frOpn_{134–153}$, containing the RGD and the SLAYGLR integrin binding motifs, either intact or scrambled (31), were used with OVA to induce tolerance in mice, allowing us to unveil the involvement of the different integrin-binding motifs of Opn in pDC recruitment (Fig. 8A). $frOpn_{134–153}$ represents the thrombin cleaved fragment of Opn that reveals the otherwise cryptic domain SLAYGLR (28). OVA/frOpn1, containing an intact SLAYGLR motif but a scrambled RGD motif, induced the accumulation of higher numbers of pDCs in LNs compared with OVA and OVA/rOpn (Fig. 8A). Conversely, frOpn2, which contains an intact RGD, but a scrambled SLAYGLR motif, induced a reduction in pDC numbers in dLNs compared with all other treatments (Fig. 8A). When both motifs were scrambled, as in the case of frOpn3, the numbers and percentages of pDCs were not significantly altered compared with OVA (Fig. 8A, Supplemental Fig. 3A). OVA/frOpn1 induced higher percentages of pDCs in dLNs compared with OVA and OVA/frOpn3 (Supplemental Fig. 3A). These data revealed that the Opn SLAYGLR motif is responsible for pDC accumulation in dLNs. These data also reveal that the RGD motif suppresses this accumulation.

To examine the in vivo tolerogenic potential of frOpn1 in allergic disease, mice were treated with OVA, together with frOpn1 or frOpn3 for control, before the induction of allergic airway inflammation (Fig. 8B). OVA/frOpn1 was more successful than OVA/frOpn3 in promoting tolerance and, thus, protecting mice against allergic airway inflammation, as demonstrated by lower Penh values (Fig. 8C). BAL eosinophilia, as well as inflammatory score and mucus staining, was also dampened after OVA/frOpn1 treatment (Fig. 8D). In addition, treatment with OVA/frOpn1 led to reduced levels of OVA-specific responses (Fig. 8E) and numbers of T1ST2$^+$CD4$^+$ T cells in dLNs (Fig. 8D). Collectively, this dataset indicates that the Opn SLAYGLR motif significantly boosts tolerance.

Opn SLAYGLR motif induces IFN-β expression in pDCs

We further asked whether OVA/frOpn1 treatment affects in vivo pDC immune profile 36–40 h after tolerance induction (Fig. 3A). In vitro, OVA/frOpn1 conditioning of pDCs promoted a 2-fold increase in *Ifnb* mRNA expression at 16 h (Fig. 9A). The observed difference in *Ifnb* expression was also reflected in the amount of IFN-β secreted, which was 5-fold higher in OVA/frOpn1-conditioned pDCs compared with OVA/frOpn3-conditioned pDCs (Fig. 9B). House dust mite endotoxin-free Derp1 was also used to test whether the increased IFN-β

Downloaded from http://www.jimmunol.org/ by guest on January 17, 2018

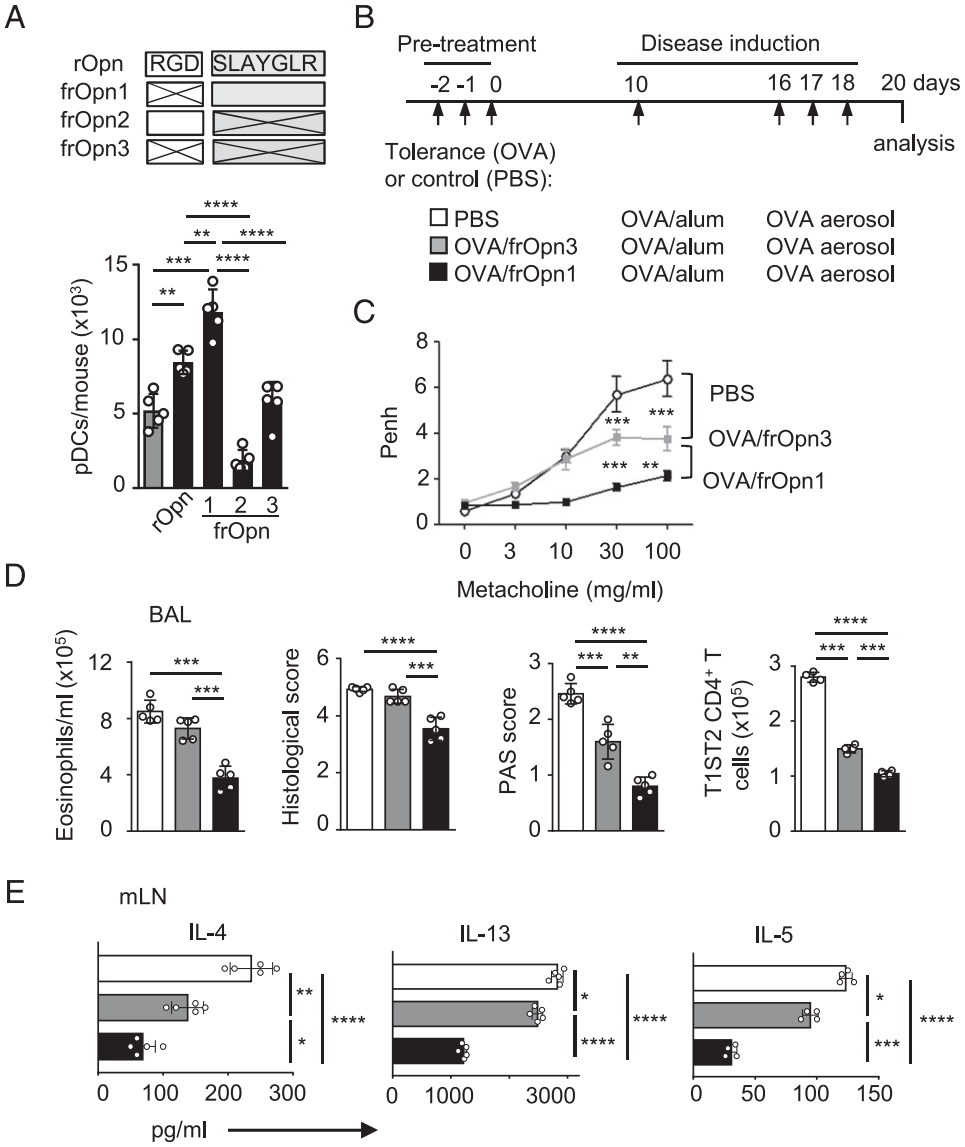

FIGURE 8. Opn SLAYGLR motifs boost tolerance by enhancing pDC recruitment to protect from allergy. (**A**) Numbers of dLN 7AAD$^-$ CD11c$^+$B220$^+$PDCA1$^+$Siglec-H$^+$ pDCs after 40 h of tolerance induction with EndoGrade OVA i.n., along with rOpn, frOpn1, frOpn2, frOpn3, or PBS (as in Fig. 3A). (**B**) Mice were treated with OVA/frOpn during tolerance induction before allergic airway disease induction in (**C**)–(**E**). Control mice were pretreated with PBS, and allergy was subsequently induced (white bars). (C) AHR (depicted as Penh) at day 19. (D) Eosinophil cell count in BAL, histological assessment of lung inflammation (H&E scoring) and lung mucus production (PAS score), and numbers of T1ST2$^+$CD4$^+$ T$_H$2 cells in mLNs. (E) Levels of IL-4, IL-5, and IL-13 in supernatants of OVA-stimulated mLN cells. The same numbers of pooled mLN cells were cultured in four to six different wells per group. Data are mean ± SEM (n = 5, mice per group), one representative of three independent experiments. *$p \leq 0.0332$, **$p \leq 0.0021$, ***$p \leq 0.0002$, ****$p < 0.0001$.

response could be observed using another allergen. Indeed, Derp1/frOpn1 in vitro–conditioning of pDCs resulted in higher *Ifnb* expression compared with Derp1/frOpn3 (Fig. 9C). We also measured higher levels of *Ifnb* expression in OVA/rOpn-conditioned pDCs compared with OVA/PBS-conditioned pDCs (Supplemental Fig. 3B).

RNA expression analysis using mLN pDCs isolated from mice treated with OVA versus OVA/rOpn showed differential expression of *Ifnb* compared to mice treated with OVA (data not shown). We found that, indeed, *Ifnb* expression was upregulated in mLN pDCs isolated from mice treated with OVA/frOpn1 compared with those isolated from mice treated with OVA/frOpn3 (Fig. 9E). To confirm the changes in IFN-β expression in vivo, we used IFN-β^{EYFP} reporter mice. OVA/frOpn1-tolerized mice had significantly increased numbers of IFN-β^{EYFP+} pDCs and higher IFN-β expression per pDC (mean fluorescence intensity [MFI]) compared with OVA/frOpn3-tolerized mice (Fig. 9D). To test whether this effect is relevant to the Ag used, we tolerized IFN-β^{EYFP} mice with a self-antigen, MOG$_{35–55}$, with frOpn1 or frOpn3. MOG$_{35–55}$/frOpn1 administration to IFN-β^{EYFP} mice resulted in significantly increased accumulation of IFN-β^{EYFP+} pDCs and IFN-β expression per pDC (MFI) in LNs (Fig. 9F). However, the increase was modest compared with Opn/OVA, possibly because MOG is a peptide. These results suggest that, under tolerogenic conditions, the Opn SLAYGLR motif can boost *Ifnb* expression in pDCs through a mechanism independent of the Ag used.

Opn/SLAYGLR-induced IFN-β in pDCs is protective against allergic disease

pDCs were primed in vitro with endotoxin-free OVA and frOpn1 or frOpn3 and transferred into mice prior to induction of allergic airway inflammation (Fig. 10A). Recipient mice were *Ifnar1*$^{+/+}$ or *Ifnar1*$^{-/-}$. pDCs treated with frOpn1 were significantly more potent at protecting *Ifnar1*$^{+/+}$ mice against allergic airway inflammation, as demonstrated by reduced lung airway inflammation, BAL eosinophilia, and goblet cell hyperplasia, compared with the control and OVA groups (Fig. 10A). Similar enhanced protection was also observed when pDCs were treated with rOpn and adoptively transferred into *Ifnar1*$^{+/+}$ mice (Fig. 7B–D). Actually, type I IFN produced by pDCs was crucial in maintaining this protective effect, because *Ifnar1*$^{-/-}$ recipient mice were not protected against allergic asthma (Fig. 10A). These results demonstrate that the integrin-binding SLAYGLR domain of Opn renders pDCs more regulatory through type I IFN production in the context of allergic airway inflammation. In fact, pDCs cannot

Downloaded from http://www.jimmunol.org/ by guest on January 17, 2018

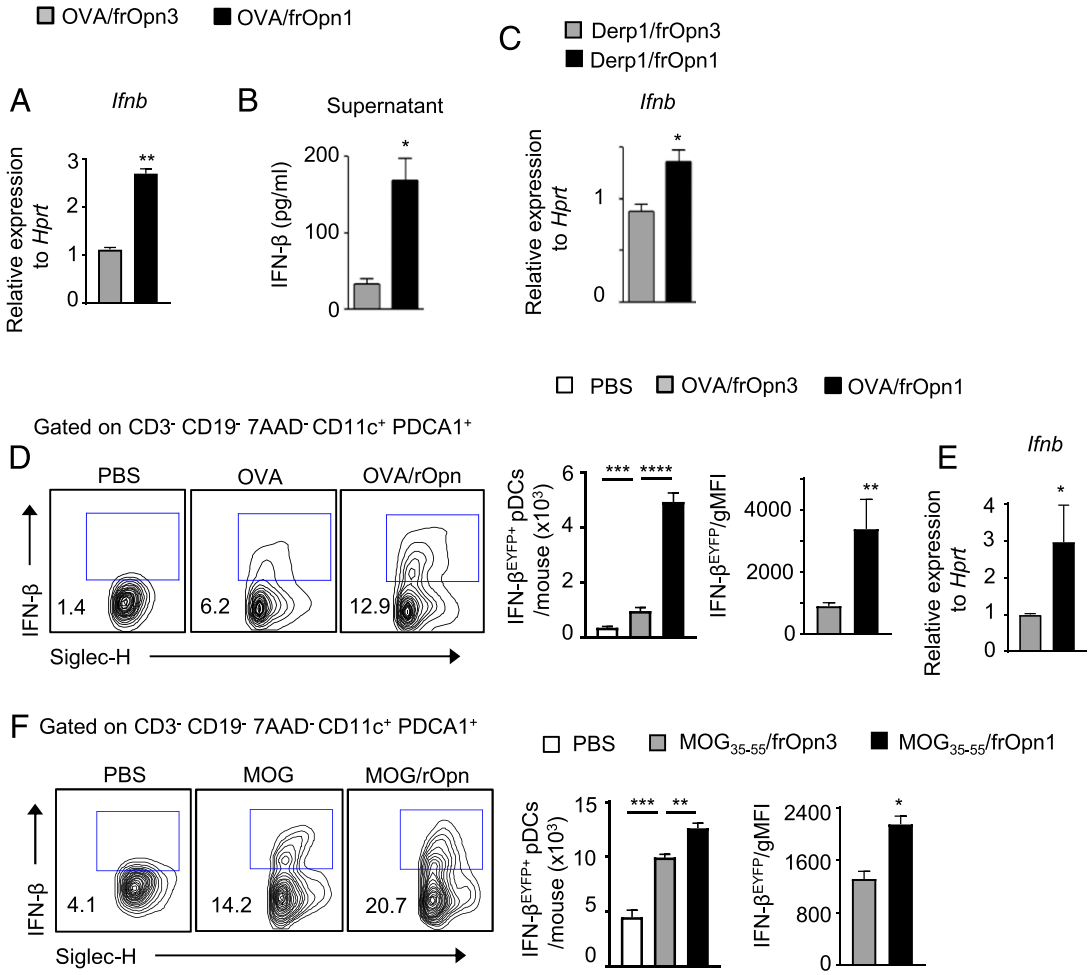

FIGURE 9. Opn SLAYGLR motif induces IFN-β production from pDCs. (**A**) Relative *Ifnb* expression to *Hprt* in pDCs conditioned in vitro with OVA/frOpn1 or OVA/frOpn3. (**B**) Levels of IFN-β in the supernatants of the same cultures. (**C**) Relative *Ifnb* expression to *Hprt* in pDCs conditioned in vitro with Derp1/frOpn1 compared with Derp1/frOpn3. (**D**) Representative percentages in flow cytometric plots and numbers of 7AAD$^-$CD3$^-$CD19$^-$CD11c$^+$PDCA-1$^+$Siglec-H$^+$IFN-β^{EYFP+} pDCs in dLNs of PBS-treated or OVA-tolerized mice and geometrical MFI (gMFI) of IFN-β-expressing pDCs. (**E**) Relative *Ifnb* expression to *Hprt* in pDCs isolated from dLNs of OVA/frOpn3- and OVA/frOpn1-tolerized mice. (**F**) Representative percentages in flow cytometric plots and numbers of total 7AAD$^-$CD3$^-$CD19$^-$CD11c$^+$PDCA-1$^+$Siglec-H$^+$IFN-β^{EYFP+} pDCs and gMFI of IFN-β–expressing pDCs in dLNs of mice treated with PBS or tolerized with $MOG_{35–55}$/frOpn3 or $MOG_{35–55}$/frOpn1. Mice were tolerized as in Fig. 3A. Data are mean ± SEM (n = 6–8 mice per group), pooled data from three independent experiments. *$p \leq 0.0332$, **$p \leq 0.0021$, ***$p \leq 0.0002$, ****$p < 0.0001$.

preserve their regulatory function in recipients that lack expression of type I IFNR. Finally, neutralization of IFNAR1 during the OVA tolerance-induction phase (Fig. 10B) resulted in reduced protection from allergic airway disease concomitant with increased eosinophilia in BAL (Fig. 10C) and increased OVA-specific responses (Fig. 10D). This indicates that type I IFN is absolutely necessary for effective antigenic tolerance induction in this context.

Discussion

In this article, we unveil a new role for Opn, and particularly its SLAYGLR motif, in setting up a tolerogenic milieu driving antigenic tolerance induction and, thus, leading to protection from allergic airway inflammation.

The respiratory mucosa is constantly being exposed to a myriad of nonpathogenic environmental Ags. To protect against the immunopathological consequences of this constant stimulus, a default low noninflammatory T_H2 mechanism and/or a T cell–mediated tolerance mechanism is activated (53). The mechanism underlying these processes is not fully understood. In this study, we initially demonstrate that Opn induces tolerance by tilting the pDC/cDC balance in favor of anti-inflammatory pDCs, via differentially regulating their CCR7 expression. CCR7-dependent homing of DCs into dLNs is required for the induction of tolerance (50).

Opn promotes T_H2 effector responses when administered during the allergen-sensitization phase (5). In contrast, we have previously shown that Opn inhibits T_H2 responses during allergen challenge, and administration of rOpn during that phase is suppressive for experimental allergic asthma (5). In this study, we explore the role of Opn during a different phase, which is when Ag is administered during tolerance induction, prior to sensitization. Thus, Opn is administered i.n., prior to the sensitization phase, along with the allergen (antigen), to test its effects upon antigenic tolerance induction. Together, our results from this study, as well as from a previous study (5), show that administration of Opn during antigenic tolerance induction and during antigenic challenge is protective and, thus, can be used as a preventive or a therapeutic agent against allergic airway disease.

Regulatory cytokines, such as *Tgfb1*, *Il10*, and *Fgl2*, and molecules, such as *Ido* (54), were substantially upregulated in our Opn-driven tolerance model, creating an immunoregulatory microenvironment in the dLN. This tolerogenic milieu was

Downloaded from http://www.jimmunol.org/ by guest on January 17, 2018

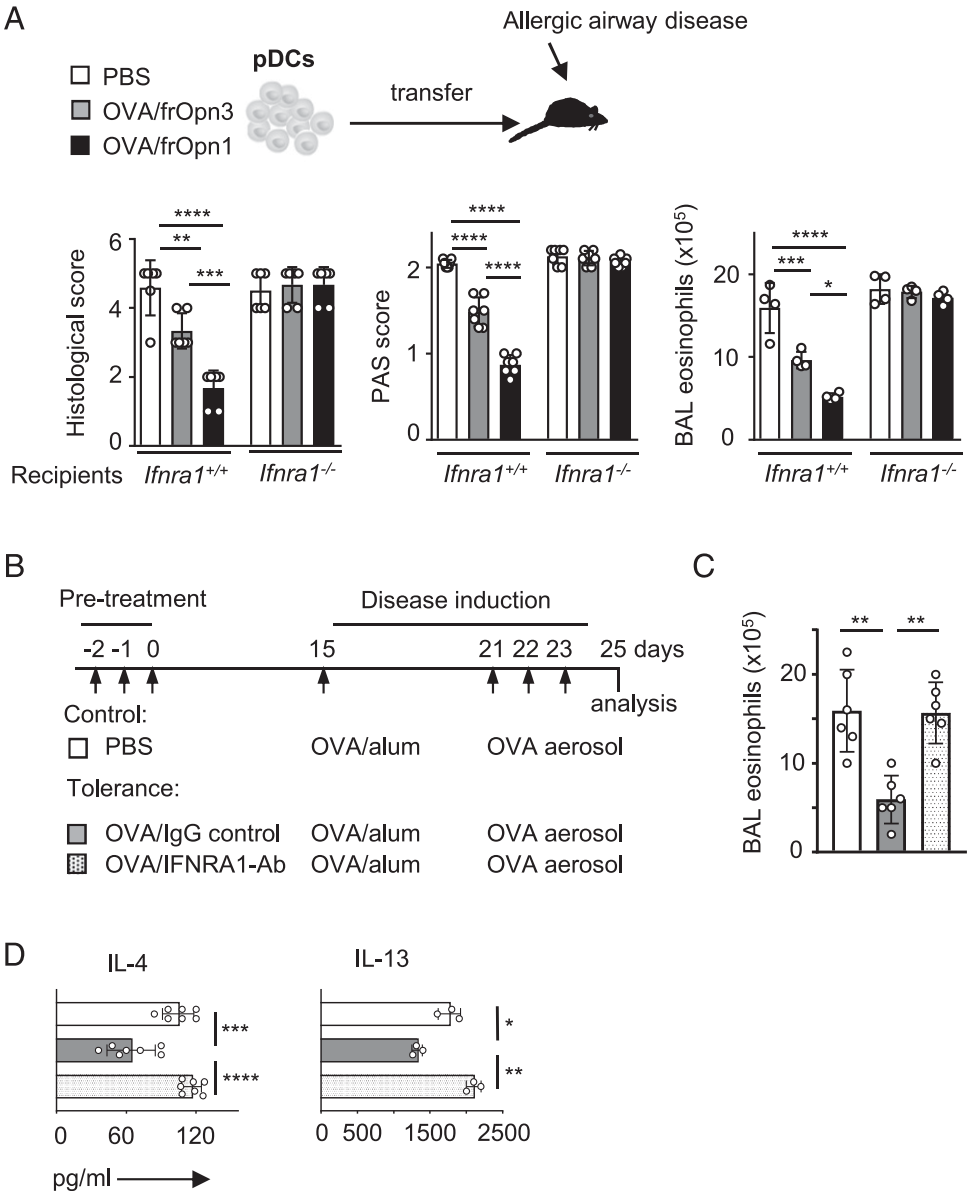

FIGURE 10. Opn/SLAYGLR-induced IFN-β in pDCs renders them protective against allergic disease. (**A**) Isolated *Ifnar1*$^{+/+}$ pDCs were primed in vitro with OVA and frOpn1 or frOpn3 or with PBS and adoptively transferred to *Ifnar1*$^{+/+}$ or *Ifnar*$^{-/-}$ mice. Histological scores for airway inflammation and goblet cell hyperplasia in lung sections stained with H&E and PAS, respectively, and number of eosinophils present in BAL. (**B**) OVA tolerance induction with the use of blocking Ab against IFNAR1 or isotype control prior to allergic airway disease induction. Control mice were pretreated with PBS prior to allergic airway disease induction (white bars). (**C**) Numbers of eosinophils in BAL and (**D**) levels of IL-4 and IL-13 in supernatants of OVA-stimulated dLN cells. The same numbers of pooled mLN cells were cultured in three or seven different wells per group. Data are mean ± SEM [$n = 4$ or 5 mice per group (A) and $n = 6$ mice per group (B–D)], one representative of three independent experiments. *$p \leq 0.0332$, **$p \leq 0.0021$, ***$p \leq 0.0002$, ****$p < 0.0001$.

accompanied by the accumulation of Foxp3$^+$ Treg cells, which are very important for induction of tolerance (51). Mice that had enhanced Treg cell numbers due to rOpn administration showed suppressed effector responses and were protected from allergic disease. When Foxp3$^+$ Treg cells were depleted, Opn-mediated tolerance boosting was abolished. In light of its well-established proinflammatory function (10–12), it was unexpected that Opn could be an inducer of Treg cell accumulation in vivo. In the absence of pDCs, rOpn administration was no longer capable of inducing increased numbers of Foxp3$^+$ Treg cells in dLNs, demonstrating that rOpn affects Treg cell numbers primarily through its impact on pDCs. In contrast, after tolerance induction without the addition of Opn, Treg cell numbers do not appear to depend on pDCs, because pDC depletion did not reduce their numbers. These results show that rOpn conditions pDCs to enhance Treg cell accumulation. Functional flexibility and fostering of Treg cell responses are typical features of pDC involvement in tolerance (4, 46), as also revealed by our studies.

Thrombin cleavage of Opn occurs during homeostatic and inflammatory conditions (24, 25), and conformational changes after thrombin cleavage result in higher-affinity binding to certain receptors (26). In fact, the cryptic SLAYGLR motif is revealed upon thrombin cleavage of Opn, which is vital for its interaction with α9β1 integrin (28). Because the SLAYGLR motif of Opn protein interacts with α4β1, α4β7, and α9β1 integrins (12), and the RGD motif interacts with the αvβ3 integrin (11, 12), we used synthetic frOpn$_{134–153}$, containing both integrin binding motifs (intact or scrambled) (31). Thrombin cleavage of Opn also produces a fragment containing the C-terminal half of Opn, which interacts with certain CD44 variants (12, 27). In our settings, as well as in other settings (31, 55, 56), frOpn$_{134–153}$ has a greater efficiency

Downloaded from http://www.jimmunol.org/ by guest on January 17, 2018

compared with full-length Opn. Thus, it is possible that interaction of Opn with CD44 interferes with certain Opn effects, such as pDC recruitment. Future investigations will elucidate the role of Opn–CD44 interactions in tolerance induction.

Under endotoxin-free conditions, we demonstrated that the SLAYGLR domain of Opn (frOpn1) enhances IFN-β expression in pDCs exposed to protein or peptide Ag. Accordingly, we showed that adoptively transferred OVA/frOpn1-treated pDCs were more efficient at suppressing allergic airway inflammation in recipient mice. This regulatory function was indeed mediated by the observed upregulated production of IFN-β by pDCs, because *Ifnar1*$^{-/-}$ recipient mice were not protected against allergic asthma. During the course of allergic airway inflammation, pDCs, as well as their type I IFN production, are suppressive for disease (4, 57–59). Our studies reveal that pDCs expressing higher IFN-β levels due to exposure to Opn are important for protective tolerance prior to disease induction. Importantly, our experiments point to a crucial role for type I IFNs during the induction of efficient antiallergic antigenic tolerance. Accordingly, IFNAR signaling promotes Treg cell development and function under stress conditions (60).

Opn administered during tolerance also resulted in a remarkable upregulation of the ligands of CCR7, CCL19, and CCL21 in dLNs, reminiscent of that observed in tumors (61). Specifically, high CCL21 expression by melanoma in mice was associated with an immunotolerant microenvironment, which included the induction of lymphoid-like reticular stromal networks, an altered cytokine milieu, and, most importantly, the recruitment of regulatory leukocyte populations (61). High Opn expression is prevalent in many types of malignancy (62); although Opn is considered proinflammatory, most of these tumors escape immune surveillance. Thus, it is possible that Opn and its mediated induction of CCL21 could also be involved in suppression of antitumor immunity.

In this article, we demonstrate that the SLAYGLR motif of sOpn enhances regulatory mechanisms when administered together with endotoxin-free Ag in a tolerogenic context. In this respect, Opn has a unique effect on immunity, differing substantially from its effects in the presence of danger signals. The SLAYGLR motif of Opn interacts with integrins (12). Addressing which integrin mediates the tolerogenic effects of the SLAYGLR motif of Opn on Ag-loaded pDCs, and primarily the induction of IFN-β, will assist in the design of therapies targeting tolerance in allergy. Finally, our results point to novel effects of Opn on Foxp3^{+} Treg cells that remain to be explored.

Acknowledgments

We thank M. Bessa, M. Willart, M. Plantiga, K. Vergote, S. De Prijck, and M. Van Heerswinghel for assisting with experiments and K. Deswarte and A. Apostolidou for flow cytometric sorting of cellular populations. We thank Amgen and Celldex Therapeutics for kindly providing recombinant human Flt3 ligand.

Disclosures

The authors have no financial conflicts of interest.

References

1. Lambrecht, B. N., and H. Hammad. 2015. The immunology of asthma. *Nat. Immunol.* 16: 45–56.
2. Lloyd, C. M., and C. M. Hawrylowicz. 2009. Regulatory T cells in asthma. *Immunity* 31: 438–449.
3. Palomares, O., M. Martín-Fontecha, R. Lauener, C. Traidl-Hoffmann, O. Cavkaytar, M. Akdis, and C. A. Akdis. 2014. Regulatory T cells and immune regulation of allergic diseases: roles of IL-10 and TGF-β. *Genes Immun.* 15: 511–520.
4. de Heer, H. J., H. Hammad, T. Soullié, D. Hijdra, N. Vos, M. A. Willart, H. C. Hoogsteden, and B. N. Lambrecht. 2004. Essential role of lung plasmacytoid dendritic cells in preventing asthmatic reactions to harmless inhaled antigen. *J. Exp. Med.* 200: 89–98.
5. Xanthou, G., T. Alissafi, M. Semitekolou, D. C. Simoes, E. Economidou, M. Gaga, B. N. Lambrecht, C. M. Lloyd, and V. Panoutsakopoulou. 2007. Osteopontin has a crucial role in allergic airway disease through regulation of dendritic cell subsets. *Nat. Med.* 13: 570–578.
6. Oriss, T. B., M. Ostroukhova, C. Seguin-Devaux, B. Dixon-McCarthy, D. B. Stolz, S. C. Watkins, B. Pillemer, P. Ray, and A. Ray. 2005. Dynamics of dendritic cell phenotype and interactions with CD4+ T cells in airway inflammation and tolerance. *J. Immunol.* 174: 854–863.
7. Akbari, O., and D. T. Umetsu. 2005. Role of regulatory dendritic cells in allergy and asthma. *Curr. Allergy Asthma Rep.* 5: 56–61.
8. Corry, D. B., and F. Kheradmand. 2005. The future of asthma therapy: integrating clinical and experimental studies. *Immunol. Res.* 33: 35–52.
9. Hawrylowicz, C. M., and A. O'Garra. 2005. Potential role of interleukin-10-secreting regulatory T cells in allergy and asthma. *Nat. Rev. Immunol.* 5: 271–283.
10. O'Regan, A. W., G. J. Nau, G. L. Chupp, and J. S. Berman. 2000. Osteopontin (Eta-1) in cell-mediated immunity: teaching an old dog new tricks. *Immunol. Today* 21: 475–478.
11. Chabas, D., S. E. Baranzini, D. Mitchell, C. C. Bernard, S. R. Rittling, D. T. Denhardt, R. A. Sobel, C. Lock, M. Karpuj, R. Pedotti, et al. 2001. The influence of the proinflammatory cytokine, osteopontin, on autoimmune demyelinating disease. *Science* 294: 1731–1735.
12. Wang, K. X., and D. T. Denhardt. 2008. Osteopontin: role in immune regulation and stress responses. *Cytokine Growth Factor Rev.* 19: 333–345.
13. Murugaiyan, G., A. Mittal, and H. L. Weiner. 2010. Identification of an IL-27/osteopontin axis in dendritic cells and its modulation by IFN-gamma limits IL-17-mediated autoimmune inflammation. *Proc. Natl. Acad. Sci. USA* 107: 11495–11500.
14. Shinohara, M. L., J. H. Kim, V. A. Garcia, and H. Cantor. 2008. Engagement of the type I interferon receptor on dendritic cells inhibits T helper 17 cell development: role of intracellular osteopontin. *Immunity* 29: 68–78.
15. Kourepini, E., N. Paschalidis, D. C. Simoes, M. Aggelakopoulou, J. L. Grogan, and V. Panoutsakopoulou. 2016. TIGIT enhances antigen-specific Th2 recall responses and allergic disease. *J. Immunol.* 196: 3570–3580.
16. Shinohara, M. L., L. Lu, J. Bu, M. B. Werneck, K. S. Kobayashi, L. H. Glimcher, and H. Cantor. 2006. Osteopontin expression is essential for interferon-alpha production by plasmacytoid dendritic cells. *Nat. Immunol.* 7: 498–506.
17. Renkl, A. C., J. Wussler, T. Ahrens, K. Thoma, S. Kon, T. Uede, S. F. Martin, J. C. Simon, and J. M. Weiss. 2005. Osteopontin functionally activates dendritic cells and induces their differentiation toward a Th1-polarizing phenotype. *Blood* 106: 946–955.
18. Kawamura, K., K. Iyonaga, H. Ichiyasu, J. Nagano, M. Suga, and Y. Sasaki. 2005. Differentiation, maturation, and survival of dendritic cells by osteopontin regulation. *Clin. Diagn. Lab. Immunol.* 12: 206–212.
19. Ashkar, S., G. F. Weber, V. Panoutsakopoulou, M. E. Sanchirico, M. Jansson, S. Zawaideh, S. R. Rittling, D. T. Denhardt, M. J. Glimcher, and H. Cantor. 2000. Eta-1 (osteopontin): an early component of type-1 (cell-mediated) immunity. *Science* 287: 860–864.
20. Murugaiyan, G., A. Mittal, and H. L. Weiner. 2008. Increased osteopontin expression in dendritic cells amplifies IL-17 production by CD4+ T cells in experimental autoimmune encephalomyelitis and in multiple sclerosis. *J. Immunol.* 181: 7480–7488.
21. Uede, T. 2011. Osteopontin, intrinsic tissue regulator of intractable inflammatory diseases. *Pathol. Int.* 61: 265–280.
22. Gerstenfeld, L. C. 1999. Osteopontin in skeletal tissue homeostasis: an emerging picture of the autocrine/paracrine functions of the extracellular matrix. *J. Bone Miner. Res.* 14: 850–855.
23. Chiodoni, C., M. P. Colombo, and S. Sangaletti. 2010. Matricellular proteins: from homeostasis to inflammation, cancer, and metastasis. *Cancer Metastasis Rev.* 29: 295–307.
24. Grassinger, J., D. N. Haylock, M. J. Storan, G. O. Haines, B. Williams, G. A. Whitty, A. R. Vinson, C. L. Be, S. Li, E. S. Sørensen, et al. 2009. Thrombin-cleaved osteopontin regulates hemopoietic stem and progenitor cell functions through interactions with alpha9beta1 and alpha4beta1 integrins. *Blood* 114: 49–59.
25. Yamamoto, N., F. Sakai, S. Kon, J. Morimoto, C. Kimura, H. Yamazaki, I. Okazaki, N. Seki, T. Fujii, and T. Uede. 2003. Essential role of the cryptic epitope SLAYGLR within osteopontin in a murine model of rheumatoid arthritis. *J. Clin. Invest.* 112: 181–188.
26. Lund, S. A., C. M. Giachelli, and M. Scatena. 2009. The role of osteopontin in inflammatory processes. *J. Cell Commun. Signal.* 3: 311–322.
27. Weber, G. F., S. Ashkar, M. J. Glimcher, and H. Cantor. 1996. Receptor-ligand interaction between CD44 and osteopontin (Eta-1). *Science* 271: 509–512.
28. Yokosaki, Y., N. Matsuura, T. Sasaki, I. Murakami, H. Schneider, S. Higashiyama, Y. Saitoh, M. Yamakido, Y. Taooka, and D. Sheppard. 1999. The integrin alpha(9)beta (1) binds to a novel recognition sequence (SVVYGLR) in the thrombin-cleaved amino-terminal fragment of osteopontin. *J. Biol. Chem.* 274: 36328–36334.
29. Leavenworth, J. W., B. Verbinnen, J. Yin, H. Huang, and H. Cantor. 2015. A p85α-osteopontin axis couples the receptor ICOS to sustained Bcl-6 expression by follicular helper and regulatory T cells. *Nat. Immunol.* 16: 96–106.
30. Marson, A., K. Kretschmer, G. M. Frampton, E. S. Jacobsen, J. K. Polansky, K. D. MacIsaac, S. S. Levine, E. Fraenkel, H. von Boehmer, and R. A. Young. 2007. Foxp3 occupancy and regulation of key target genes during T-cell stimulation. *Nature* 445: 931–935.
31. Kourepini, E., M. Aggelakopoulou, T. Alissafi, N. Paschalidis, D. C. Simoes, and V. Panoutsakopoulou. 2014. Osteopontin expression by CD103- dendritic cells drives intestinal inflammation. *Proc. Natl. Acad. Sci. USA* 111: E856–E865.
32. van Rijt, L. S., S. Jung, A. Kleinjan, N. Vos, M. Willart, C. Duez, H. C. Hoogsteden, and B. N. Lambrecht. 2005. In vivo depletion of lung CD11c+ dendritic cells during allergen challenge abrogates the characteristic features of asthma. *J. Exp. Med.* 201: 981–991.
33. Asselin-Paturel, C., G. Brizard, J. J. Pin, F. Brière, and G. Trinchieri. 2003. Mouse strain differences in plasmacytoid dendritic cell frequency and function revealed by a novel monoclonal antibody. *J. Immunol.* 171: 6466–6477.

Downloaded from http://www.jimmunol.org/ by guest on January 17, 2018

34. Swiecki, M., S. Gilfillan, W. Vermi, Y. Wang, and M. Colonna. 2010. Plasmacytoid dendritic cell ablation impacts early interferon responses and antiviral NK and CD8(+) T cell accrual. *Immunity* 33: 955–966.
35. McMillan, S. J., G. Xanthou, and C. M. Lloyd. 2005. Manipulation of allergen-induced airway remodeling by treatment with anti-TGF-beta antibody: effect on the Smad signaling pathway. *J. Immunol.* 174: 5774–5780.
36. Semitekolou, M., T. Alissafi, M. Aggelakopoulou, E. Kourepini, H. H. Kariyawasam, A. B. Kay, D. S. Robinson, C. M. Lloyd, V. Panoutsakopoulou, and G. Xanthou. 2009. Activin-A induces regulatory T cells that suppress T helper cell immune responses and protect from allergic airway disease. *J. Exp. Med.* 206: 1769–1785.
37. Naik, S. H., P. Sathe, H. Y. Park, D. Metcalf, A. I. Proietto, A. Dakic, S. Carotta, M. O'Keeffe, M. Bahlo, A. Papenfuss, et al. 2007. Development of plasmacytoid and conventional dendritic cell subtypes from single precursor cells derived in vitro and in vivo. *Nat. Immunol.* 8: 1217–1226.
38. Panoutsakopoulou, V., M. E. Sanchirico, K. M. Huster, M. Jansson, F. Granucci, D. J. Shim, K. W. Wucherpfennig, and H. Cantor. 2001. Analysis of the relationship between viral infection and autoimmune disease. *Immunity* 15: 137–147.
39. Humbles, A. A., C. M. Lloyd, S. J. McMillan, D. S. Friend, G. Xanthou, E. E. McKenna, S. Ghiran, N. P. Gerard, C. Yu, S. H. Orkin, and C. Gerard. 2004. A critical role for eosinophils in allergic airways remodeling. *Science* 305: 1776–1779.
40. Dahl, M. E., K. Dabbagh, D. Liggitt, S. Kim, and D. B. Lewis. 2004. Viral-induced T helper type 1 responses enhance allergic disease by effects on lung dendritic cells. *Nat. Immunol.* 5: 337–343.
41. Hansen, G., G. Berry, R. H. DeKruyff, and D. T. Umetsu. 1999. Allergen-specific Th1 cells fail to counterbalance Th2 cell-induced airway hyperreactivity but cause severe airway inflammation. *J. Clin. Invest.* 103: 175–183.
42. Krug, N., J. Madden, A. E. Redington, P. Lackie, R. Djukanovic, U. Schauer, S. T. Holgate, A. J. Frew, and P. H. Howarth. 1996. T-cell cytokine profile evaluated at the single cell level in BAL and blood in allergic asthma. *Am. J. Respir. Cell Mol. Biol.* 14: 319–326.
43. Osorio, F., C. Fuentes, M. N. López, F. Salazar-Onfray, and F. E. González. 2015. Role of dendritic cells in the induction of lymphocyte tolerance. *Front. Immunol.* 6: 535.
44. Maldonado, R. A., and U. H. von Andrian. 2010. How tolerogenic dendritic cells induce regulatory T cells. *Adv. Immunol.* 108: 111–165.
45. Wakkach, A., N. Fournier, V. Brun, J. P. Breittmayer, F. Cottrez, and H. Groux. 2003. Characterization of dendritic cells that induce tolerance and T regulatory 1 cell differentiation in vivo. *Immunity* 18: 605–617.
46. Swiecki, M., and M. Colonna. 2010. Unraveling the functions of plasmacytoid dendritic cells during viral infections, autoimmunity, and tolerance. *Immunol. Rev.* 234: 142–162.
47. Takagi, H., T. Fukaya, K. Eizumi, Y. Sato, K. Sato, A. Shibazaki, H. Otsuka, A. Hijikata, T. Watanabe, O. Ohara, et al. 2011. Plasmacytoid dendritic cells are crucial for the initiation of inflammation and T cell immunity in vivo. *Immunity* 35: 958–971.
48. Förster, R., A. C. Davalos-Misslitz, and A. Rot. 2008. CCR7 and its ligands: balancing immunity and tolerance. *Nat. Rev. Immunol.* 8: 362–371.
49. Platt, A. M., and G. J. Randolph. 2013. Dendritic cell migration through the lymphatic vasculature to lymph nodes. *Adv. Immunol.* 120: 51–68.
50. Worbs, T., and R. Förster. 2007. A key role for CCR7 in establishing central and peripheral tolerance. *Trends Immunol.* 28: 274–280.
51. Weiner, H. L., A. P. da Cunha, F. Quintana, and H. Wu. 2011. Oral tolerance. *Immunol. Rev.* 241: 241–259.
52. Lahl, K., C. Loddenkemper, C. Drouin, J. Freyer, J. Arnason, G. Eberl, A. Hamann, H. Wagner, J. Huehn, and T. Sparwasser. 2007. Selective depletion of Foxp3+ regulatory T cells induces a scurfy-like disease. *J. Exp. Med.* 204: 57–63.
53. Holt, P. G., D. H. Strickland, M. E. Wikström, and F. L. Jahnsen. 2008. Regulation of immunological homeostasis in the respiratory tract. *Nat. Rev. Immunol.* 8: 142–152.
54. Shevach, E. M. 2009. Mechanisms of foxp3+ T regulatory cell-mediated suppression. *Immunity* 30: 636–645.
55. Albertsson, A. M., X. Zhang, J. Leavenworth, D. Bi, S. Nair, L. Qiao, H. Hagberg, C. Mallard, H. Cantor, and X. Wang. 2014. The effect of osteopontin and osteopontin-derived peptides on preterm brain injury. *J. Neuroinflammation* 11: 197.
56. Doyle, K. P., T. Yang, N. S. Lessov, T. M. Ciesielski, S. L. Stevens, R. P. Simon, J. S. King, and M. P. Stenzel-Poore. 2008. Nasal administration of osteopontin peptide mimetics confers neuroprotection in stroke. *J. Cereb. Blood Flow Metab.* 28: 1235–1248.
57. Farkas, L., E. O. Kvale, F. E. Johansen, F. L. Jahnsen, and F. Lund-Johansen. 2004. Plasmacytoid dendritic cells activate allergen-specific TH2 memory cells: modulation by CpG oligodeoxynucleotides. *J. Allergy Clin. Immunol.* 114: 436–443.
58. Fonseca, D. E., and J. N. Kline. 2009. Use of CpG oligonucleotides in treatment of asthma and allergic disease. *Adv. Drug Deliv. Rev.* 61: 256–262.
59. Matsui, H., H. Tomizawa, K. Eiho, Y. Kashiwazaki, S. Edwards, M. Biffen, J. P. Bell, A. Bahl, A. J. Leishman, C. M. Murray, et al. 2012. Mechanism of action of inhibition of allergic immune responses by a novel antedrug TLR7 agonist. *J. Immunol.* 189: 5194–5205.
60. Metidji, A., S. A. Rieder, D. D. Glass, I. Cremer, G. A. Punkosdy, and E. M. Shevach. 2015. IFN-α/β receptor signaling promotes regulatory T cell development and function under stress conditions. *J. Immunol.* 194: 4265–4276.
61. Shields, J. D., I. C. Kourtis, A. A. Tomei, J. M. Roberts, and M. A. Swartz. 2010. Induction of lymphoidlike stroma and immune escape by tumors that express the chemokine CCL21. *Science* 328: 749–752.
62. Shevde, L. A., S. Das, D. W. Clark, and R. S. Samant. 2010. Osteopontin: an effector and an effect of tumor metastasis. *Curr. Mol. Med.* 10: 71–81.

Downloaded from http://www.jimmunol.org/ by guest on January 17, 2018

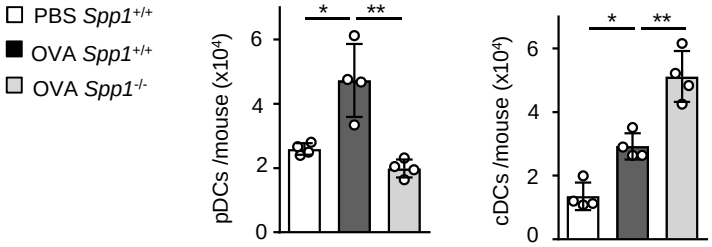

Supplemental Figure 1. Opn increases the numbers of pDCs. Mice were pretreated with endotoxin-free OVA or PBS and analyzed after 40 hrs as in Figure 3a. Numbers of 7AAD^{-}CD3^{-}CD19^{-}CD11c^{+}CD11b^{-}B220^{+}PDCA-1^{+} pDCs in dLNs and 7AAD^{-}CD11c^{+}CD11b^{+}PDCA-1^{-} cDCs from dLNs of *Spp1*$^{+/+}$ or *Spp1*$^{-/-}$ mice. Values are expressed as mean ± SEM (*n*=4 mice per group), one representative experiment of three independent experiments.

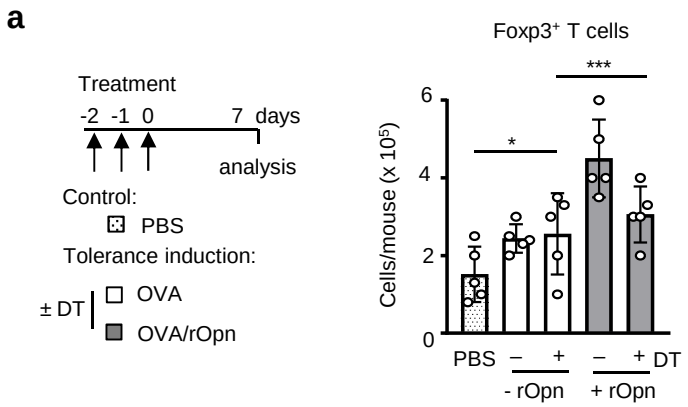

Supplemental Figure 2. pDC deletion in BDCA2-DTR mice abrogates Treg cell accumulation in Opn-induced tolerance. For pDC depletion mice received diphtheria toxin (DT) on days -4, -3 followed by tolerance induction for Treg cell generation. Control mice were treated with PBS. Numbers of Treg cell ($CD3^+CD4^+Foxp3^+$) accumulation in dLNs with and without rOpn administration. Values are expressed as mean ± SEM (*n*=5 mice per group), one representative experiment of three independent experiments.

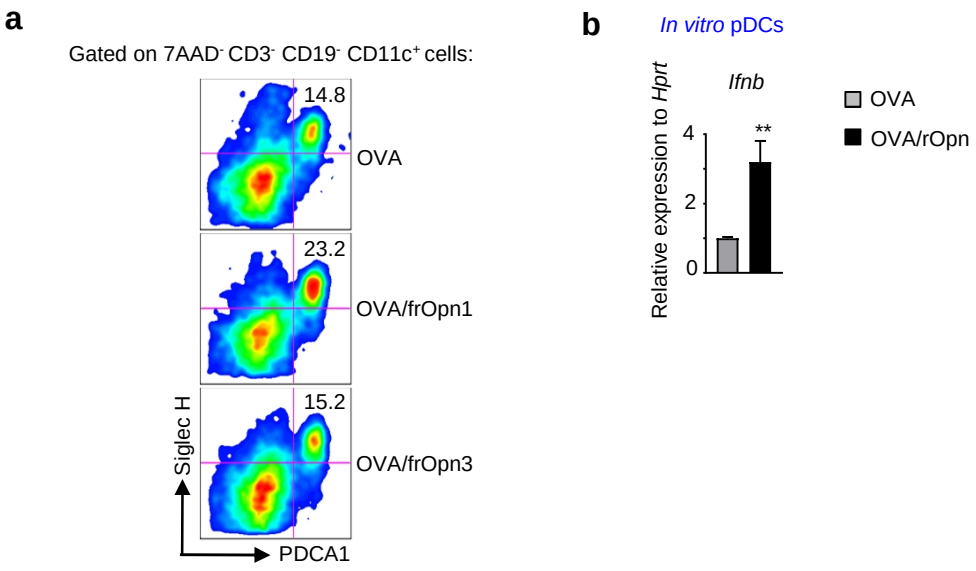

Supplemental Figure 3. Opn SLAYGR motif enhances pDC recruitment in dLNs and IFN-β production in pDCs. (A) Gating strategy and percentages of 7AAD^{-}CD3^{-}CD19^{-}CD11c^{+}PDCA-1^{+}Siglec-H^{+} pDCs in dLNs of tolerized mice treated with OVA or OVA/frOpn1 or OVA/frOpn3 (scrambled peptide: see Fig. 8A) for control. Mice were tolerized as in Fig. 3A. **(B)** Relative *Ifnb* expression to *Hprt* in pDCs conditioned *in vitro* with OVA and OVA/rOpn. Values are expressed as mean ± SEM (n=10), pooled data from three independent experiments.

Gene:	Sense (5'-3')	anti-sense (5'-3)
Ccl19	ATCTGAGCGATTCCAGTCA	TCTTCCGCATCATTAGCAC
Ccl21	TTCACGGTCCAACTCACA	CTCTTTCTTCTGACTCTCTA
Fgl2	ACAGCCGAGGACAGTAGA	CGGTTAGATTTGCCACTTTG
Ido	GGCTTCTTCCTCGTCTCTCT	ATTTCCTTGGCTTTCTCCAG
Tgfb1	CCTGGGTTGGAAGTGGA	TAGTAGACGATGGGCAGT
Ifnb	CCTATGGAGATGACGGAGAA	TGGAGAGCAGTTGAGGACAT

Supplemental Table 1: Primers used for real-time PCR.